Science of the Total Environment 612 (2018) 1030–1041

Contents lists available at ScienceDirect

Science of the Total Environment

journal homepage: www.elsevier.com/locate/scitotenv

# Are optical indices good proxies of seasonal changes in carbon fluxes and stress-related physiological status in a beech forest?

E. Nestola [a,b,*], A. Scartazza [a,c,**], D. Di Baccio [c], A. Castagna [d], A. Ranieri [d], M. Cammarano [c], F. Mazzenga [b,c], G. Matteucci [e], C. Calfapietra [a,f]

[a] Institute of Agroenvironmental and Forest Biology, National Research Council of Italy (CNR), Via Marconi 2, 05010 Porano, TR, Italy
[b] Department for Innovation in Biological, Agro-Food and Forest Systems (DIBAF), University of Tuscia, Via S. Camillo de Lellis snc, 01100 Viterbo, Italy
[c] Institute of Agroenvironmental and Forest Biology, National Research Council of Italy (CNR), Via Salaria km 29,300, 00016, Monterotondo Scalo, Roma, RM, Italy
[d] Department of Agriculture, Food and Environment, University of Pisa, via del Borghetto 80, 56124 Pisa, Italy
[e] Institute for Agriculture and Forestry Systems in the Mediterranean, National Research Council of Italy (CNR), Via Patacca, 85 I-80056 Ercolano, NA, Italy
[f] Czechglobe, Global Change Research Institute, Academy of Sciences of the Czech Republic, Brno, Czech Republic

## HIGHLIGHTS

- Hot and dry summer impaired carbon fluxes in a beech forest.
- Chlorophyll indices are good proxies of changes in NEE during stress periods.
- Carotenoid indices track plant physiological status and response to stress.
- Methodological integrated approach explains forest conditions and functionality.

## GRAPHICAL ABSTRACT

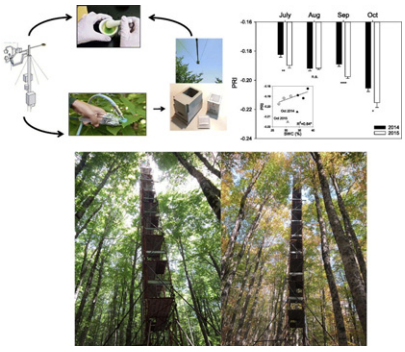


## ARTICLE INFO

*Article history:*
Received 13 April 2017
Received in revised form 15 August 2017
Accepted 15 August 2017
Available online 7 September 2017

*Keywords:*
Chlorophyll fluorescence
*Fagus sylvatica* L.
Heat stress
Net ecosystem exchange

## ABSTRACT

This study investigates the functionality of a Mediterranean-mountain beech forest in Central Italy using simultaneous determinations of optical measurements, carbon (C) fluxes, leaf eco-physiological and biochemical traits during two growing seasons (2014–2015). Meteorological variables showed significant differences between the two growing seasons, highlighting a heat stress coupled with a reduced water availability in mid-summer 2015. As a result, a different C sink capacity of the forest was observed between the two years of study, due to the differences in stressful conditions and the related plant physiological status. Spectral indices related to vegetation (VIs, classified in *structural*, *chlorophyll* and *carotenoid* indices) were computed at top canopy level and used to track $CO_2$ fluxes and physiological changes. Optical indices related to structure (EVI 2, RDVI, DVI and MCARI 1) were found to better track Net Ecosystem Exchange (NEE) variations for 2014, while indices related to chlorophylls (SR red edge, CL red edge, MTCI and DR) provided better results for 2015. This suggests that when

*Abbreviations:* A, antheraxanthin; C, carbon; Car, carotenoids; Car/Chl tot, carotenoids/Chl tot ratio; Chl, chlorophyll; Chl *a*, chlorophyll *a*; Chl *b*, chlorophyll *b*; Chl tot, total chlorophyll (Chl *a* + Chl *b*); DEPS, de-epoxidation index; EC, eddy covariance; ETR, electron transport rate; fAPAR, fraction of absorbed photosynthetically active radiation; GPP, gross primary productivity; LAI, leaf area index; N, nitrogen; NPQ, non-photochemical quenching; NEE, net ecosystem exchange; NIR, near infrared reflectance; PAR, photosynthetically active radiation; $P_{June + July}$, cumulative precipitation for June and July; PPFD, photosynthetic photon flux density; PSII, photosystem II; $\Phi_{PSII}$, quantum yield of PSII in light adapted state; SWC, soil water content; $T_{July}$, average temperature for the month of July; V, violaxanthin; VAZ, xanthophyll-cycle pigment pool; VI, vegetation index; VPD, vapor pressure deficit; Z, zeaxanthin.

* Correspondence to: E. Nestola, Department for Innovation in Biological, Agro-Food and Forest Systems (DIBAF), University of Tuscia, Via S. Camillo de Lellis snc, 01100 Viterbo, Italy.
** Correspondence to: A. Scartazza, Institute of Agroenvironmental and Forest Biology, National Research Council of Italy (CNR), Via Salaria km 29,300, 00016, Monterotondo Scalo, Roma, RM, Italy.
*E-mail addresses:* enrica.nestola@ibaf.cnr.it (E. Nestola), andrea.scartazza@ibaf.cnr.it (A. Scartazza).

http://dx.doi.org/10.1016/j.scitotenv.2017.08.167

Photosynthetic pigments
Proximal sensing

environmental conditions are not limiting for forest sink capacity, structural parameters are more strictly connected to C uptake, while under stress conditions indices related to functional features (e.g., chlorophyll content) become more relevant. *Chlorophyll* indices calculated with red edge bands (SR red edge, NDVI red edge, DR, CL red edge) resulted to be highly correlated with leaf nitrogen content ($R^2 > 0.70$), while weaker, although significant, correlations were found with chlorophyll content. *Carotenoid* indices (PRI and PSRI) were strongly correlated with both chlorophylls and carotenoids content, suggesting that these indices are good proxies of the shifting pigment composition related to changes in soil moisture, heat stress and senescence. Our work suggests the importance of integrating different methods as a successful approach to understand how changing climatic conditions in the Mediterranean mountain region will impact on forest conditions and functionality.



## 1. Introduction

Exploring biomes under natural stress conditions is a research priority to quantify their contribution to C balance. During the last decades, several methods have been used to monitor ecosystem C uptake such as, for instance, leaf and branch gas exchange (Long and Bernacchi, 2003), sap-flow technique (Scott et al., 2006), plant harvesting (Gower et al., 1999), remote (Garbulsky et al., 2013; Huemmrich et al., 2010) and proximal sensing (Sakowska et al., 2014), eddy covariance (EC) technique (Papale et al., 2006) and models (Coops et al., 2009; Le Maire et al., 2005). Among these, the simultaneous use of EC fluxes with remote sensing allows to compare C fluxes at high temporal resolution with information at a broader spatial scale, thus reducing the weaknesses of the two techniques and generating a solid integrated dataset (Gamon et al., 2010). However, even if flux measurements and remote sensing are able to broadly characterize the ecosystem productivity, the mechanistic details operating at finer temporal and spatial scales need further investigations. Thus, the integration of proximal sensing techniques at flux tower sites may currently represent a tool to understand physiological details operating at finer temporal and spatial scales (Gamon, 2015). In this context of integrated approaches, the "ground truthing" at ecosystem and leaf level is needed as validation of optical measurements in their ability to monitor the seasonal variability in the ecosystem physiological status. Fluorescence based parameters and pigment analyses can be used as ground methods to verify the accuracy of data collected from different sources. Chlorophyll (Chl) fluorescence represents a powerful tool to obtain detailed information on the efficiency of photochemistry and heat dissipation capacity (Maxwell and Johnson, 2000), by which plants respond to environmental changes (Murchie and Lawson, 2013). Likewise, the measurement of changes in pigment pools are essential for testing, validating or estimating optical indices (Stylinski et al., 2002) and fluorescence (Zarco-Tejada et al., 2003).

In this framework of different approaches to monitor vegetation condition and assess primary productivity, the application of visible and near infrared reflectance (NIR) developed during the last 30 years allows to assess plant status and recognize the vegetation characteristics from spectral signature (Ollinger, 2011). Normalized Difference Vegetation Index (NDVI) (Rouse et al., 1974) and Enhanced Vegetation Index (EVI) (Huete et al., 2002), less affected by saturation issues, were extensively used for global vegetation monitoring. The traditional broadband greenness indices measure green biomass and are mostly useful to track the changes of photosynthetic activity just during the plant growth and senescence period (Gamon et al., 1995). They were commonly used as proxy for Leaf Area Index (LAI) (Wu et al., 2010a), fraction of Absorbed Photosynthetically Active Radiation (fAPAR) (Nestola et al., 2016), green biomass (Pettorelli et al., 2005) and as input in satellite based diagnostic models (Dong et al., 2015). These structural indices are mostly affected by the variations of canopy architecture (Haboudane et al., 2004) but can fail in predicting changes in pigment composition, as reflectance in visible bands (i.e., red) saturates at relatively low Chl contents. Consequently, other indices have been explored using very informative features of the red edge region, which corresponds to the increase of reflectance at the boundary between the Chl absorption in the red wavelengths and leaf scattering in the NIR wavelengths. For instance, NDVI red edge (Gitelson and Merzlyak, 1994) and Cl red edge (Gitelson et al., 2005), both including red edge (690–750 nm) wavelengths in their formulation, provide not only better predictions of leaf Chl content (Sims and Gamon, 2002) but also effective proxies for remote estimation of gross primary productivity (GPP) (Wu et al., 2009). Chlorophylls were not the only pigment cluster considered to study pigment effects on leaf optical properties. Carotenoids, anthocyanins and other pigments were also investigated and a variety of optical indices were developed to track their content (Merzlyak et al., 2003). Among these, the Photochemical Reflectance Index (PRI) (Gamon et al., 1992), related to the xanthophyll cycle activity, is used as a proxy of light-use efficiency (Garbulsky et al., 2011). The responsiveness of reflectance indices to changes in pigments and fluorescence may provide accurate estimates of seasonal changes in the photosynthetic flux of vegetation. In view of all these considerations, Vegetation Indices (VIs) have the potentiality to be essential tools in the assessment of primary production and of other canopy attributes, including the detection of stress response (Glenn et al., 2008).

Considering their C sink potential, climate change mitigation capacity and socioeconomic impact, beech forests represent one of the most important ecosystems in Europe (Danielewska et al., 2013; Pötzelsberger et al., 2015). Hence, investigating changes in plant ecophysiology and monitoring productivity is a relevant concern from both an ecological and an economic point of view. When performed in a mature forest and in natural conditions, these studies are generally difficult due to the high canopies, and installing sensors for proximal sensing can represent an effective approach to monitor canopy functionality under different meteorological and phenological conditions. This work used an integrated approach in order to: i) monitor seasonal variations of C fluxes, photosynthetic pigment pools and Chl fluorescence and their relationships with optical indices; ii) assess which optical indices act as the best proxies for monitoring C flux dynamics in a forest subjected to natural seasonal changes, mainly related to variations in soil water availability, temperature and vapor pressure deficit; iii) evaluate which optical indices can detect the shifting in photosynthetic pigment composition associated with stress events and with the senescence phase in healthy and stressed vegetation.

## 2. Materials and methods

### 2.1. Study site and experimental design

The experiment was carried out at the Collelongo-Selvapiana pure beech forest (Abruzzo region, Central Italy, 41°50′58″N, 13°35′17″E, 1560 m elevation). The site is equipped with a 28 m scaffold tower geared towards measuring ecosystem $H_2O$ and $CO_2$ since 1993 using the eddy-covariance technique (Matteucci et al., 2007). The site is part of the LTER, FluxNet and ICP-Forests network and it is included in a wider forest area, in the external belt of the Abruzzo-Lazio-Molise National Park and its structure and conditions are representative of Central Apennine beech forests (Scartazza et al., 2004). Vegetation is

homogeneous and dominated by European beech (*Fagus sylvatica* L.). In the area of the experimental site, plant density is 740 trees $ha^{-1}$ (including trees with 1 cm diameter at 1.30 m height), the basal area is 42.2 $m^2$ $ha^{-1}$ with a mean diameter at breast height of 25.5 cm and a mean height of 20.7 m. Mean diameter and height of the dominant trees is 45 cm and 27 m, respectively (data are from the periodic 5-year stand survey performed in 2012). At the peak of the growing season, LAI in 2014–2015 was 5.5–5.9 $m^2$ $m^{-2}$ (Scartazza et al., 2016). A detailed description of the site, instrumental set-up, soil characteristics and stand structure is reported in previous works (Guidolotti et al., 2013; Matteucci et al., 2007; Nestola et al., 2017; Scartazza et al., 2013). The climate is the Mediterranean montane, with fresh to moderately warm summer and cold winters. Mean annual temperature and precipitation measured at the site for the period 1996–2015 are 6.9 °C and 1116 mm, respectively. Soil Water Content (SWC) is measured continuously with the Time domain Reflectometry technique using a profile of 4 CS616 probes (Campbell Scientific Inc., Logan, Utah, USA) installed at 20 cm soil depth. For the years under study (2014 and 2015), data on air temperature, precipitations, SWC and Vapor Pressure Deficit (VPD) are reported in Fig. 1. Measurements described in this study started in June 2014 and ended in October 2015, including almost entirely the two growing seasons. Four datasets using different techniques were collected: 1) C fluxes; 2) optical indices; 3) Chl fluorescence and 4) photosynthetic pigment contents. While $CO_2$ fluxes and vegetation reflectance were monitored continuously, fluorescence and pigments were sampled at least once a month in both growing seasons. Details on sampling layout are provided separately in the following sections.

### 2.2. Flux measurements and meteorological data

Ecosystem $CO_2$ and $H_2O$ fluxes were measured following the EUROFLUX (Aubinet et al., 1999) and then the FluxNet methodology. The experimental set-up consists of a fast-response infrared gas analyzer (LI-7000, LI-COR, Lincoln, NE, USA) and a three-dimensional sonic anemometer (CSAT3, Campbell Scientific, Logan, UT, USA). Air was drawn through the analyzer by a pump (VDO M48 × 25/l, Antriebstechinik GmbH, Germany) installed downstream of the analyzer. Raw data (20 Hz) and basic means (30 min) were stored in a data logger (CR1000, Campbell Scientific). Raw EC data were analyzed using the software package EddyPro (LI-COR, v. 5.2.1) to calculate corrected vertical fluxes of $CO_2$ and $H_2O$, using standard corrections, including data-quality check. All fluxes were calculated according to the standardised approaches of FluxNet. More details are reported in Mazzenga (2017).

For this study, daily estimates of Net Ecosystem Exchange (NEE, $gC\ m^{-2}\ d^{-1}$, including the storage component) were used. Data are presented following the EC convention, where negative values indicate $CO_2$ absorbed from the atmosphere (i.e. a sink for carbon). When one or more half-hourly data were missing or their quality was not acceptable, gap-filling techniques were used to obtain a complete data set. To present a complete seasonal trend, all NEE data were used. However, for correlation analysis among fluxes, ecophysiological parameters and optical indices, NEE values with a quality flag lower than 0.65 (on average, about 20% of data) were discarded, in order to use more reliable and effectively measured data. Along with EC fluxes, the main meteorological variables were measured every 10 s and averaged (or summed) over 30 min including photosynthetically active radiation (PAR), air temperature, soil temperature and soil water content, precipitation and other radiation parameters. Details on meteorological measurements set-up have been presented elsewhere (Guidolotti et al., 2013; Matteucci et al., 2007; Scartazza et al., 2016, 2013).

### 2.3. Optical measurements

The tower was equipped with a multispectral radiometer system MSR16R (CROPSCAN, Inc., Rochester, USA) which was mounted on a metal pole (6 m) on the last floor of the flux tower (28 m) in late June 2014. The radiometer accommodated 14 wavebands (14 up and 14 down sensor band pairs; Supplemental content, Table S1), which concurrently measured the reflecting and incoming radiation. Data collected were stored in the data logger controller (DLC). Downward looking sensors had a 28° field of view (FOV) and detected reflected radiance in the wavebands reported in Table S1, while the incident irradiance (IRR) was measured through a flashed, opal glass, cosine diffuser.

Since the diameter of the field of view is half of the height of the radiometer over the target, the down-facing sensors received direct reflected irradiance from surfaces within a circular conic region having 14 m of diameter. In complex canopy ecosystems like forests, reflected irradiance could arrive from leaves not too far below the radiometer or leaves much lower, when there are openings below the radiometer. Spectral data were collected during the growing seasons 2014 and 2015; the spectral indices computed in this work come from data recorded from July to October of both years. The radiometer was set in a standalone operation collecting optical measurements daily from 6:00

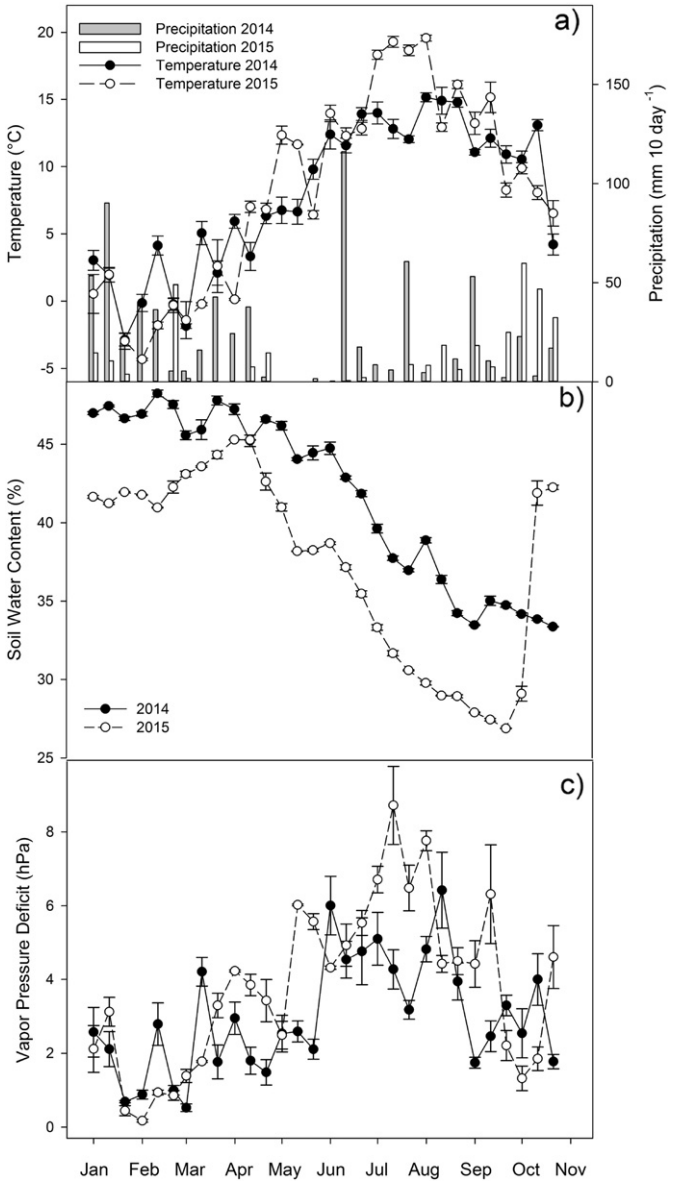


**Fig. 1.** Seasonal variations of air temperature (T) and precipitation (a), Soil Water Content (SWC) determined at 20 cm of soil depth (b) and Vapor Pressure Deficit (VPD) (c) in Collelongo beech forest. Data of T, SWC and VPD are presented as 10-days period averages ± standard error, while precipitation is presented as cumulative value of each 10-days period.

**Table 1**
Vegetation indices computed in this study. R stands for reflectance and the following number indicates the given wavelengths.

| Vegetation index | Formula | Reference |
|---|---|---|
| *Structural indices* | | |
| Simple Ratio (SR) | R750 / R670 | (Jordan, 1969) |
| Enhanced Vegetation Index 2 (EVI 2) | 2.5 × (R750 − R670) / (R750 + 2.4 × R670 + 1.0) | (Jiang et al., 2008) |
| Difference Vegetation Index (DVI) | R 750 − R 670 | (Tucker, 1979) |
| Normalized Difference Vegetation Index (NDVI) | (R750 − R670) / (R750 + R670) | (Rouse et al., 1974) |
| Renormalized Difference Vegetation Index (RDVI) | (R750 − R670) / (R750 + R670) × 1/2 | (Haboudane et al., 2004) |
| Modified Chlorophyll Absorption Ratio Index (MCARI 1) | 1.2 × [2.5 × (R750 − R670) − 1.3 × (R750 − R550)] | (Haboudane et al., 2004) |
| Modified Simple Ratio (MSR) | (R 750 / R 670 − 1) / (R 750 / R 670 + 1) × 1/2 | (Haboudane et al., 2004) |
| Optimized Soil-Adjusted Vegetation Index (OSAVI) | (1.16) × (R750 − R670) / (R750 + R670 + 0.16) | (Rondeaux et al., 1996) |
| Wide Dynamic Range Vegetation Index (WDRVI) | (0.1 × R750 − R670) / (0.1 × R750 + R670) | (Gitelson, 2004) |
| *Chlorophyll indices* | | |
| Simple Ratio red edge (SR red edge) | R750 / R710 | (Zarco-Tejada et al., 2001) |
| Simple Ratio green (SR green) | R750 / R550 | (Gitelson and Merzlyak, 1997) |
| NDVI red edge | (R750 − R720) / (R750 + R720) | (Gitelson and Merzlyak, 1994) |
| Red edge chlorophyll index (Cl red edge) | (R750 / R720) − 1 | (Gitelson et al., 2003) |
| NDVI green | (R750 − R550) / (R750 + R550) | (Gitelson et al., 1996) |
| Green chlorophyll index (Cl green) | (R750 / R550) − 1 | (Gitelson, 2003) |
| MCARI 2 | [(R750 − R720) − 0.2 × (R750 − R550)] (R750 / R720) | (Wu et al., 2009) |
| Transformed Chlorophyll Absorption Ratio Index (TCARI) | 3[(R720 − R670) − 0.2× (R720 − R550) × (R720 / R670)] | (Haboudane et al., 2002) |
| MERIS terrestrial chlorophyll index (MTCI) | (R750 − R720) / (R720 − R670) | (Dash and Curran, 2004) |
| Difference Ratio (DR) | (R750 − R720) / (R750 − R681) | (Datt, 1999) |
| *Carotenoid indices* | | |
| Carotenoid Reflectance Index (CRI) | (1 / R510) − (1 / R550) | (Gitelson et al., 2002) |
| Photochemical Reflectance Index (PRI) | (R530 − R570) / (R530 + R570) | (Gamon et al., 1992) |
| Structure Insensitive Pigment Index (SIPI 2) | (R750 − R550) / (R750 − R670) | (Blackburn, 1998) |
| Plant Senescence Reflectance Index (PSRI) | (R670 − R510) / R750 | (Merzlyak et al., 1999) |

to 18:00. Downward irradiance and upward radiance were stored every 10 min. In this study, only scans that met the criteria IRR ≥ 300 W/m$^2$ and Sun angles ≤ 50° were considered. The Cropscan multispectral radiometer reflectance was calculated as the ratio between downward and upward sensor readings. Sensor temperature corrections, up-sensor cosine response correction and radiometric calibration constants were applied before the final calculation. In order to reduce solar angle effects, reflectance data from 11:00 to 13:00 (local solar time) were selected to compute the VIs indices (Table 1) used in our analysis. In this study, we considered three main categories of VIs related to: i) canopy structure (*structural* indices); ii) biochemistry (*chlorophyll* indices) and iii) plant physiology/stress (*carotenoid* indices).

### 2.4. Leaf level measurements

During 2014 and 2015, several field campaigns were carried out from spring to autumn in order to collect different kind of leaf level measurements and compare data between the growing seasons of the two study-years: 1) Chl fluorescence, 2) photosynthetic pigment content and 3) nitrogen content (N, % or cg g$^{-1}$). Samples were collected within 2 h from solar noon, to reduce diurnal variability during the sampling periods and to allow correlation between the biochemical and the optical measurements (see Section 2.3). We selected six trees having branches accessible from the flux tower at 24-26 m (top of the canopy). In each campaign, at least four branches from four different trees were labelled, cut and immediately soaked in the water for sampling. Leaves were kept as close to their original orientation as possible to maintain the original illumination conditions during sampling. For each branch, at least three leaves were randomly selected and labelled. The leaf scale measurements were performed on the selected leaves (at least three) for every branch ($n$ = 12–18): fluorescence measurements were carried out on one half of each sampled leaf, while pigment analyses on the other half of the same leaf. For pigments analysis, each leaf sample was kept separate, immediately packed in aluminum paper, frozen in liquid $N_2$ and then preserved at −80 °C until analysis. For N analysis, sampled leaves (including the half leaves used for fluorescence measurements) were pooled for each branch, packed and stored into labelled paper bags. On these pooled leaves (half and intact leaves), for a total of at least 5–15 leaves for each branch (4–6), N determination was performed. More details are provided in the following sections.

### 2.5. Fluorescence measurements

Fluorescence parameters were monitored on fully expanded leaves of the upper part of the canopy using a miniaturized pulse amplitude-modulated fluorometer (Mini-PAM; Heinz Walz GmbH, Effeltrich, Germany) between 10:00 and 12:00. The fluorometer fibre optic was kept at a fixed angle to ensure measurements repeatability, and on average 20 leaves were sampled for each campaign.

The quantum yield of PSII in light adapted state ($\Phi_{PSII}$), an indicator of the photosynthetic efficiency of photosystem II, was obtained as:

$$\Phi_{PSII} = \frac{\Delta F}{F'_m} = \frac{F'_m - F}{F'_m} \quad (1)$$

where Fm′ is the maximum fluorescence yield with all the PSII reaction centres in the reduced state obtained by superimposing a saturating light flash during exposure to actinic light and F is the fluorescence yield at the actual reduction state of PSII reaction centres during actinic illumination.

The electron transport rate (ETR) (μmol m$^{-2}$ s$^{-1}$), which provided a more direct estimation related to photosynthetic activity (Baker, 2008), was calculated based on chlorophyll fluorescence measurement of $\Phi_{PSII}$ parameter, employing the following equation:

$$ETR = \Phi_{PSII} \times PPFD \times 0.5 \times 0.84 \quad (2)$$

where incident photosynthetic photon flux density (PPFD) was obtained by a PAR quantum sensor positioned at measurements position (Fig. 5a, insert), 0.5 is a factor that accounts for the partitioning of energy between PSII and PSI and 0.84 is the leaf absorbance coefficient (Maxwell and Johnson, 2000).

Non-photochemical quenching (NPQ) was calculated according to the Stern-Volmer equation as reported by Bilger and Björkman (1990):

$$NPQ = \frac{(F_m - F'_m)}{F'_m} \quad (3)$$

where Fm is the maximum fluorescence yield in the dark-adapted leaves (about 30 min) after application of a saturation flash of light that completely closes all the PSII reaction centres.

### 2.6. Pigment determinations

The speciation of photosynthetic pigments was performed according to the method reported by Castagna et al. (2013) and modified in Di Baccio et al. (2014). Samples from leaves (half part) previously utilized for fluorescence measurements were frozen in liquid $N_2$ and stored at −80 °C until use. Frozen samples (~190 mg, fresh weight) were homogenized under dimmed room light in 100% HPLC-grade acetone with 1 mM Na-ascorbate, filtered through 0.2-μm filters (Sartorius Stedim Biotech, Goettingen, Germany) and immediately analyzed. The analysis was performed by HPLC (HPLC P4000, Thermo Fisher Scientific, Waltham, MA, USA) using a non-endcapped column (5 μm particle size, 250 × 4.6 mm Ø; Zorbax ODS column, Chrompack, Raritan, NJ, USA). Pigments were eluted using 100% solvent A (acetonitrile/methanol, 75/25, v/v) for the first 15 min, followed by a 2.5-min linear gradient to 100% solvent B (methanol/ethylacetate, 68/32, v/v), which continued isocratically until the end of the cycle. The separation cycle was 32 min with a flow rate of 1 mL $min^{-1}$. The column was allowed to re-equilibrate in 100% solvent A for 10 min before the next injection. Pigments (chlorophyll *a*, Chl *a*; chlorophyll *b*, Chl *b*; lutein; neoxanthin; violaxanthin, V; antheraxanthin, A; zeaxanthin, Z, and β-carotene) were detected by their absorbance at 445 nm, and quantified by injecting known amounts of pure standards (Sigma-Aldrich, Milan, Italy) into the HPLC system. The de-epoxidation index (DEPS index) of the pool of xanthophyll-cycle carotenoids (V + A + Z, VAZ) was calculated according to the following equation: [(A / 2) + Z] / (V + A + Z) × 100. The carotenoid content shown in the "Results and Discussions" section was calculated as the sum of lutein, neoxanthin, VAZ and β-carotene.

For the construction and validation of calibration curves, evaluation of total chlorophyll (Chl *a* + Chl *b*, Chl tot) and caroteinoid contents were also measured spectrophotometrically according to the method described by Wellburn (1994). Briefly, leaf tissue samples (30 mg, fresh weight) were homogenized with 80% (w/v) cold acetone, centrifuged at 10,000 ×*g* per 5 min at 4 °C, and the absorbance of the supernatant was read at 663.2, 646.8 and 470.0 nm.

### 2.7. Leaf nitrogen content

Leaf samples from each branch (5–15) of 4–6 plants were oven dried until constant weight and subsequently ground to a fine powder. About 3–4 mg of powder was used for the determination of nitrogen content (N, % or cg $g^{-1}$) using an elemental analyser (Model NA 1500, Carlo Erba, Milan, Italy).

### 2.8. Data analysis

One-way ANOVA was used to test differences in meteorological variables between 2014 and 2015. Moreover, in order to characterize the years 2014 and 2015 with respect to typical conditions at the study site, we analyzed a time series covering the period 1996–2015 measured at the site for the following variables: average temperature for the month of July ($T_{July}$), cumulative precipitation for June and July ($P_{June + July}$) and average NEE for the month of July. As a composite index for detecting situations of high temperature coupled with low precipitation the variables $T_{July}/P_{June + July}$ and $y = \log(T_{July}/P_{June + July})$ were also considered (the logarithmic transformation was used to normalize the time series). We used $P_{June + July}$ rather than $P_{July}$ alone as precipitation could have a more prolonged effect than temperature on determining stress conditions. An autoregressive model (Chatfield, 2016) was fitted to each time series (1996–2015), then measured values for the year under study were compared with model predictions.

Statistically significant differences of results from fluorescence and photosynthetic pigment measurements between 2014 and 2015 were evaluated by a two-tail *t*-test analysis ($P \leq 0.05$), conducted using STATISTICA 6.0 (StatSoft, Inc., Tulsa, OK).

A direct linear regression between spectral indices and C fluxes was assumed. The difference among the slopes and the intercepts of the relationships between VIs and NEE for different years was evaluated through analysis of covariance (ANCOVA). As ANCOVA showed significant differences between the slopes and the intercepts of each relationship, separate fits were considered for both years. Statistics for each relationship (coefficient of determination - $R^2$, root mean square error - RMSE, number of observations - *N*, probability value - *P* and Pearson correlation coefficient - *r*) were computed to evaluate the performance of the fit of the different indices. For the regressions between NEE and VIs, a common $R^2$ threshold value of 0.590 was considered for both 2014 and 2015 to identify the indices with the best performances (Table 2). Linear regressions between VIs and pigment measurements were performed by a regression analysis (determination coefficient - $R^2$ and probability value - *P*) using GraphPad Prism 6 (GraphPad Software, Inc., San Diego, CA). All the available campaigns (5 per year) were used to build the regressions shown in Table 3, while Figs. 3, 4 and 5 present only the campaigns comparable as seasonal period for both seasons of study (4 per year). The number of replicates used for analyses and correlations are specified for each data.

## 3. Results and discussions

### 3.1. Characterization of meteorological variables and temporal patterns of fluxes

Meteorological data showed broadly higher air temperature and lower precipitations during 2015 as compared to 2014 (Fig. 1a). These differences were especially evident in July, when monthly mean air temperature was 12.9 ± 2.9 °C in 2014 and 18.8 ± 1.4 °C in 2015, while monthly precipitation was 75.3 mm and 9.0 mm, respectively (Fig. 1a). Overall, the soil water content (SWC) recorded in 2015 was lower than in 2014, with the exception of a period in the first week of October (Fig. 1b). In agreement with the higher temperatures and lower SWC, higher values of vapor pressure deficit (VPD) were also reported within the growing season of 2015 (Fig. 1c). Differences between 2014 and 2015 in monthly averages of temperature, SWC and VPD for the month of July were statistically significant when tested with a simple one way ANOVA ($P < 0.0001$). The analysis of 20 years-long data series for T of July ($T_{July}$) and cumulative precipitation for June and July ($P_{June + July}$) supported the idea of particularly unfavourable (hot and dry) conditions for 2015 (Fig. S1).

The beech forest at Collelongo acted as a net $CO_2$ sink between the half of May and the last 10 days of October 2014, while in 2015 it started to be a sink from the beginning of May until middle October (Fig. 2). Over the year, the C sink capacity of the Collelongo forest was −757 gC $m^{-2}$ $y^{-1}$ in 2014 and −608 gC $m^{-2}$ $y^{-1}$ in 2015. Both opening and closing of the growing season occurred slightly earlier in 2015 as compared to 2014. The maximum net $CO_2$ uptake was recorded during the last 10 days of June for both years. From July until the beginning of August 2015 a lower sink capacity of the forest was observed as compared to the same period of 2014 (Fig. 2). This was likely due to a decrease in SWC and an increase in air temperature and VPD (Fig. 1), as also observed in a long term analysis (2000–2015) of the NEE and GPP response to air temperatures and VPD conducted on the same beech forest (Mazzenga, 2017). Our findings agree with what previously

**Table 2**
Statistics of the linear regressions between NEE and vegetation indices computed for this study. Pearson correlation coefficient ($r$), coefficient of determination ($R^2$), root mean square error (RMSE), and probability value ($P$) are presented for 2014 and 2015. Number of NEE data plotted against each optical index is 97 for 2014 and 56 for 2015. NEE is the daily NEE sum (gC $m^{-2}$ $d^{-1}$), while vegetation indices are midday averages from 11:00 to 13:00. The indices which performed $R^2 \geq 0.590$ are indicated in bold.

| | 2014 | | | | 2015 | | | |
|---|---|---|---|---|---|---|---|---|
| Vegetation indices | $r$ | $R^2$ | RMSE | $P$ value | $r$ | $R^2$ | RMSE | $P$ value |
| *Structural indices* | | | | | | | | |
| SR | −0.766 | 0.586 | 1.124 | <0.0001 | −0.611 | 0.373 | 0.961 | <0.0001 |
| **EVI 2** | **−0.818** | **0.669** | **0.025** | **<0.0001** | −0.726 | 0.527 | 0.022 | <0.0001 |
| **DVI** | **−0.804** | **0.647** | **1.849** | **<0.0001** | −0.715 | 0.512 | 1.483 | <0.0001 |
| NDVI | −0.755 | 0.570 | 0.012 | <0.0001 | −0.613 | 0.376 | 0.017 | <0.0001 |
| **RDVI** | **−0.822** | **0.675** | **0.172** | **<0.0001** | −0.726 | 0.528 | 0.158 | <0.0001 |
| **MCARI 1** | **−0.801** | **0.641** | **2.936** | **<0.0001** | −0.721 | 0.520 | 2.190 | <0.0001 |
| MSR | −0.765 | 0.585 | 0.157 | <0.0001 | −0.613 | 0.376 | 0.153 | <0.0001 |
| OSAVI | −0.759 | 0.576 | 0.014 | <0.0001 | −0.616 | 0.380 | 0.020 | <0.0001 |
| WDRVI | −0.762 | 0.581 | 0.044 | <0.0001 | −0.614 | 0.377 | 0.049 | <0.0001 |
| *Chlorophyll indices* | | | | | | | | |
| **SR red edge** | −0.750 | 0.563 | 0.277 | <0.0001 | **−0.786** | **0.617** | **0.192** | **<0.0001** |
| SR green | −0.732 | 0.535 | 0.303 | <0.0001 | −0.645 | 0.416 | 0.389 | <0.0001 |
| NDVI red edge | −0.736 | 0.541 | 0.024 | <0.0001 | −0.767 | 0.588 | 0.017 | <0.0001 |
| **CL red egde** | −0.740 | 0.547 | 0.137 | <0.0001 | **−0.771** | **0.594** | **0.085** | **<0.0001** |
| NDVI green | −0.719 | 0.517 | 0.010 | <0.0001 | −0.661 | 0.436 | 0.015 | <0.0001 |
| CL green | −0.732 | 0.535 | 0.303 | <0.0001 | −0.645 | 0.416 | 0.389 | <0.0001 |
| **MCARI 2** | **−0.795** | **0.633** | **5.020** | **<0.0001** | −0.767 | 0.589 | 3.173 | <0.0001 |
| TCARI | 0.345 | 0.119 | 1.867 | 0.0005 | 0.321 | 0.103 | 1.637 | 0.0158 |
| **MTCI** | −0.689 | 0.475 | 0.179 | <0.0001 | **−0.770** | **0.593** | **0.099** | **<0.0001** |
| **DR** | −0.693 | 0.480 | 0.025 | <0.0001 | **−0.768** | **0.590** | **0.015** | **<0.0001** |
| *Carotenoid indices* | | | | | | | | |
| CRI 550 | −0.345 | 0.119 | 0.022 | 0.0005 | −0.155 | 0.024 | 0.022 | 0.2530 |
| PRI | −0.401 | 0.161 | 0.011 | <0.0001 | −0.624 | 0.390 | 0.010 | <0.0001 |
| SIPI 2 | 0.184 | 0.034 | 0.004 | 0.0712 | −0.271 | 0.073 | 0.006 | 0.0435 |
| PSRI | 0.665 | 0.442 | 0.003 | <0.0001 | 0.445 | 0.198 | 0.007 | 0.0006 |

reported for this site (Valentini et al., 1996) and for other ecosystems located at similar latitudes, in which the net C uptake is strongly influenced by the water availability (Reichstein et al., 2007). Further statistical elaborations confirmed the effects of meteorological anomalies observed in July on NEE (Fig. S1).

### 3.2. Relations between spectral indices and NEE

Although not so extensive as in crops and grasslands (Balzarolo et al., 2015; Inoue et al., 2008; Peng et al., 2011; Sakowska et al., 2014; Wu et al., 2010a), several studies explored the relationship between $CO_2$ fluxes and VIs in mixed deciduous (Wu et al., 2010b; Xiao et al., 2004), larch (Nakaji et al., 2007) and holm oak (Garbulsky et al., 2013) forests. However, to the best of our knowledge, our study is the first one from a mature beech forest where a number of VIs are related with pigments, N content, fluorescence values and $CO_2$ fluxes. For our deciduous beech forest, the statistics of the linear regressions between daily C fluxes (NEE) versus spectral indices is reported in Table 2. Almost all regressions between VIs and NEE were highly significant ($P < 0.0001$), except for SIPI 2, CRI 550 and TCARI for both the study-years and PSRI for 2015 (Table 2).

The results suggest that, except for MCARI 2, the indices predicting best $CO_2$ fluxes in 2014 were mainly associated to canopy structure (such as RDVI, EVI 2, DVI and MCARI 1), while *chlorophyll* indices incorporating the red edge bands (such as SR red edge, CL red edge, MTCI and DR) showed better performances in 2015. The *structural* indices are generally used for the global monitoring of vegetation canopies and represent a number of alternatives to the conventional NDVI (Vescovo et al., 2012). A common feature of the *structural* indices is the use of only two spectral bands in their formulation, the red (Chl absorption region) and the NIR (region in which light is scattered by leaf mesophyll). On the other hand, *chlorophyll* indices are based on wavelengths located in the red edge region (690–750 nm) to ensure a better linearity with Chl content, and thus more suitability to follow vegetation dynamics throughout the season. Accordingly, SR red edge, CL red edge, MTCI and DR are known to provide good results in estimation of Chl content in cropland, grassland and forest canopies (Gitelson et al., 2005; Rossini et al., 2012; Zarco-Tejada et al., 2001).

The good performance of *structural* indices in 2014 suggests that the plant phenological status was the main driver of canopy physiological dynamics for that year. Differently, in the unfavourable season of 2015, high performance shown by indices in the red edge region suggests that the shifting in pigment composition associated with stress-induced changes in phenology played a relevant role as driver of seasonal C dynamics. Differences in reflectance between healthy and stressed vegetation due to changes in pigment content could be detected along the red edge (Gitelson and Merzlyak, 1996; Horler et al., 1983; Zarco-Tejada et al., 2004). In fact, a shift in the red-edge position towards shorter wavelengths has been associated to stress events inducing a decrease in chlorophyll and water contents (Rock et al., 1988), increase in fluorescence (Carter and Miller, 1994) and damage to the light harvesting structure (Meroni et al., 2009).

### 3.3. Relations between spectral indices and leaf biochemical traits

#### 3.3.1. Photosynthetic pigments and nitrogen contents

The content of total Chl (Chl $a + b$, Chl tot) of *Fagus sylvatica* L. leaves was 1.4-fold lower in July 2015 than in July 2014 (Fig. 3a). The leaf total carotenoids (Car) content (Fig. 3b) differed at the beginning (July) and at the end (October) of the two growing seasons investigated. The Car to Chl tot ratio (Car/Chl tot) was 1.6-fold higher in July 2015 than in July 2014 (Fig. 3c), while it maintained the same trend in the last part of the summer and in the autumn of the two growing seasons. The reduction in leaf Chl concentration is due to inhibition of its synthesis or to degradation under biotic and abiotic stress or senescence conditions (Cocozza et al., 2016; Hmimina et al., 2014; Scartazza et al., 2016). In our study, the leaves sampled at top-canopy level did not show visible impairments or chlorosis in July of both 2014 and 2015 years. Hence, the hot spring and early summer in 2015 (Fig. 1) probably caused the observed decrease in the total amount of Chl as compared to 2014. Moreover, the higher (1.6-fold) carotenoid levels reached in July 2015 compared to the same month of 2014 (Fig. 3b) suggests enhanced defense capabilities against heat stress through the increased synthesis of photoprotective pigments (Demmig-Adams and Adams, 2006). During the growing season, Car/Chl tot is a marker of stress of the photosystems and it is strongly related to the plant photosynthetic performance (Gamon et al., 1997), due to the antioxidant action of carotenoids and their role in the energy dissipation mechanisms (Scartazza et al., 2016). The fate and role of carotenoids during leaf senescence are not yet completely clear (Dani et al., 2016). However, it seems demonstrated that among the catabolic processes activated during the leaf senescence, there is a general degradation of pigments with a decrease of total carotenoids during leaf age progression (Procházková et al., 2009). Modifications of pigment composition are representative of the plant physiological status and are used for the estimation of both $CO_2$ uptake and radiation use efficiency through spectral indices (Gamon et al., 1997; Gamon, 2015; Gitelson et al., 2002). In this respect, Table 3 showed as both *structural* and *chlorophyll* indices reported similar $R^2$ values with Chl tot, ranging from 0.407 for MCARI 1 to 0.493 for SR red edge. As expected, relationships involving *structural* indices showed relatively low, although significant, $R^2$ values, as they are not particularly suitable to identify relatively small changes in pigment content (Zarco-Tejada et al., 2001). However, *chlorophyll* indices usually used to estimate changes in Chl content did not show the best performances (Table 3), despite what reported in literature (Main et al., 2011; Zarco-Tejada et al., 2004, 2001). This might be due to the relatively

**Table 3**
Linear regressions between optical indices and total chlorophylls (Chl tot, μg $cm^{-2}$), total carotenoids (Car, μg $cm^{-2}$) to chlorophylls ratio (Car/Chl tot), VAZ (Violaxanthin + Antheraxanthin + Zeaxanthin, μg $cm^{-2}$) pool, Electron Transport Rate (ETR, μmol $m^{-2}$ $s^{-1}$) and leaf nitrogen content (N, % or cg $g^{-1}$). Coefficient of determination ($R^2$) and probability value (*P*) are computed considering the observations (*N*) of 2014 and 2015 together. Regressions which are not statistically significant ($P \geq 0.05$) are not reported (–). Each result of pigment, nitrogen and ETR analysis used in the regressions is the average of $n = 12$–18, 40–90 and 20 leaf replicates, respectively, for every sampling campaign (5 campaigns for each year) for a total of $N = 10$ observations. Vegetation indices are midday averages from 11:00 to 13:00. The indices which performed the highest $R^2$ are indicated in bold.

| | Chl tot | | Car/Chl tot | | VAZ | | Car | | N | | ETR | |
|---|---|---|---|---|---|---|---|---|---|---|---|---|
| Vegetation indices | $R^2$ | *P* | $R^2$ | *P* | $R^2$ | *P* | $R^2$ | *P* | $R^2$ | *P* | $R^2$ | *P* |
| *Structural indices* | | | | | | | | | | | | |
| SR | 0.410 | 0.0461 | 0.500 | 0.0222 | 0.522 | 0.0183 | – | – | – | – | 0.672 | 0.0037 |
| **EVI 2** | 0.420 | 0.0427 | 0.539 | 0.0157 | 0.496 | 0.0230 | – | – | 0.553 | 0.0087 | **0.714** | **0.0021** |
| **DVI** | – | – | 0.526 | 0.0176 | 0.452 | 0.0333 | – | – | 0.541 | 0.0099 | **0.724** | **0.0018** |
| NDVI | 0.492 | 0.0239 | 0.507 | 0.0208 | 0.618 | 0.0070 | – | – | 0.600 | 0.0050 | 0.568 | 0.0118 |
| **RDVI** | 0.436 | 0.0376 | 0.542 | 0.0152 | 0.520 | 0.0186 | – | – | 0.577 | 0.0067 | **0.700** | **0.0026** |
| **MCARI 1** | 0.407 | 0.0473 | 0.540 | 0.0155 | 0.465 | 0.0299 | – | – | 0.519 | 0.0124 | **0.731** | **0.0016** |
| MSR | 0.439 | 0.0369 | 0.508 | 0.0206 | 0.558 | 0.0131 | – | – | – | – | 0.650 | 0.0048 |
| OSAVI | 0.491 | 0.0239 | 0.508 | 0.02051 | 0.617 | 0.0071 | – | – | 0.600 | 0.0051 | 0.571 | 0.0115 |
| WDRVI | 0.465 | 0.0299 | 0.512 | 0.0200 | 0.590 | 0.0095 | – | – | 0.406 | 0.0350 | 0.622 | 0.0067 |
| *Chlorophyll indices* | | | | | | | – | – | | | | |
| **SR red edge** | 0.493 | 0.0236 | **0.561** | **0.0127** | 0.661 | 0.0043 | – | – | **0.848** | <**0.0001** | 0.609 | 0.0077 |
| SR green | – | – | 0.432 | 0.0390 | 0.538 | 0.0158 | – | – | 0.576 | 0.0067 | 0.570 | 0.0116 |
| **NDVI red edge** | 0.487 | 0.0249 | 0.553 | 0.0137 | 0.606 | 0.0079 | – | – | **0.781** | **0.0003** | 0.536 | 0.0160 |
| **CL red edge** | 0.485 | 0.0252 | **0.570** | **0.0116** | 0.614 | 0.0074 | – | – | **0.724** | **0.0009** | 0.582 | 0.0103 |
| NDVI green | 0.418 | 0.0434 | 0.457 | 0.0319 | 0.579 | 0.0105 | – | – | 0.695 | 0.0014 | 0.548 | 0.0144 |
| CL green | – | – | 0.432 | 0.0390 | 0.538 | 0.0158 | – | – | 0.576 | 0.0067 | 0.570 | 0.0116 |
| **MCARI 2** | 0.437 | 0.0375 | **0.569** | **0.0117** | 0.534 | 0.0164 | – | – | 0.664 | 0.0023 | 0.675 | 0.0036 |
| **MTCI** | 0.483 | 0.0256 | **0.568** | **0.0118** | 0.607 | 0.0079 | – | – | 0.675 | 0.0019 | 0.536 | 0.0161 |
| DR | 0.459 | 0.0313 | 0.524 | 0.0179 | 0.556 | 0.0132 | – | – | **0.765** | **0.0004** | 0.467 | 0.0293 |
| *Carotenoid indices* | | | | | | | | | | | | |
| **PRI** | **0.726** | **0.0036** | 0.481 | 0.0383 | **0.800** | **0.0011** | **0.504** | **0.0322** | 0.607 | 0.0079 | – | – |
| SIPI 2 | 0.467 | 0.0293 | – | – | 0.411 | 0.0459 | – | – | – | – | – | – |
| **PSRI** | **0.588** | **0.0097** | 0.485 | 0.0252 | **0.763** | **0.0010** | **0.445** | **0.0352** | 0.542 | 0.0098 | 0.412 | 0.0454 |

limited number of observations ($N = 10$), which might be not fully representative of the heterogeneity of the canopy. Moreover, the *chlorophyll* indices as CL red edge and MCARI 2 showed high correlations with Car/Chl tot, whose importance in the plant photosynthetic activity has just been previously discussed (Gamon et al., 1997; Scartazza et al., 2016). On the other hand, no significant correlations were reported between Car and spectral indices computed in this study, with the exception for the *carotenoid* indices (i.e., PRI and PSRI) that, interestingly, exhibited also the strongest relationships with Chl tot (Table 3). In addition, the xanthophyll pool fraction (violaxanthin, antheraxanthin and zeaxanthin, VAZ) of total carotenoids showed, as expected, the highest correlations with PRI ($R^2 = 0.80$) and PSRI ($R^2 = 0.76$) and good ones

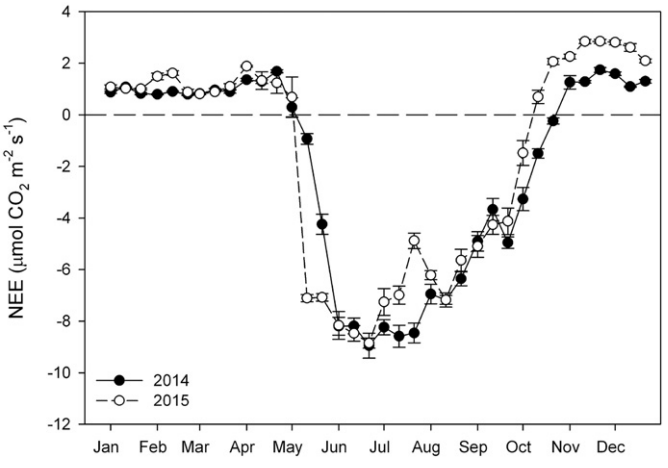


**Fig. 2.** Seasonal variations in Net Ecosystem Exchange (NEE) at Collelongo beech forest. Values of NEE are presented as 10-days period averages ± standard error.

with *structural* and *chlorophyll* indices. This confirms that the VIs investigated are not only generally correlated with the total photosynthetic pigment content, but also to pigment specificity, kind and chemical status (Gitelson et al., 2017a, 2002; Stylinski et al., 2002). In particular, as VAZ pool is associated with the photoprotection mechanisms and its size increases with increasing irradiance and environmental stress (Demming-Adams and Adams, 1996), we further investigated PSRI and PRI relationships with carotenoids in the Section 3.4.

Regarding the specificity of carotenoids, VAZ pool decreased only at the end of the growing season, with a higher DEPS index in October 2015, indicating an increasing proportion of the absorbed radiation not used for electron transport in photosynthesis (Fig. 4a). The lutein content varied only at the end of the growing season (−31% in October 2015 compared to October 2014, Fig. 4b), β-carotene was 2.4-fold higher in July and 2.5-fold lower in September 2015 than 2014 (Fig. 4c) and neoxanthin was about 1.3-fold higher in summer (July–August) 2015 than 2014 (Fig. 4d). The lutein decrease could be due to a transformation to the epoxide form to balance the excess excitation energy accumulated under stress or to a degradation in anticipated senescence processes (García-Plazaola et al., 2007; Procházková et al., 2009). The variations in β-carotene were probably induced by the activation of antioxidant defense systems (Demmig-Adams and Adams, 2006) and neoxanthin might enhance the efficiency of LHC systems, replacing the lutein epoxide and binding the VAZ components (Dall'Osto et al., 2006). In light of the above, the significant relationships of VIs with Car/Chl tot ratio were mostly driven by VAZ and other carotenoid compounds (Table 3). Indeed, neoxanthin significantly correlated with the *chlorophyll* indices DR, SR red edge, NDVI red edge and MTCI (data not shown), supporting its potential role in the photoprotective mechanisms as previously discussed.

*Chlorophyll* indices showed the strongest relationship with N content (Table 3, bold values), in agreement with other studies (Clevers and Kooistra, 2012; Ramoelo et al., 2013; Schlemmer et al., 2013), confirming the close dependence of Chl content and N status in the

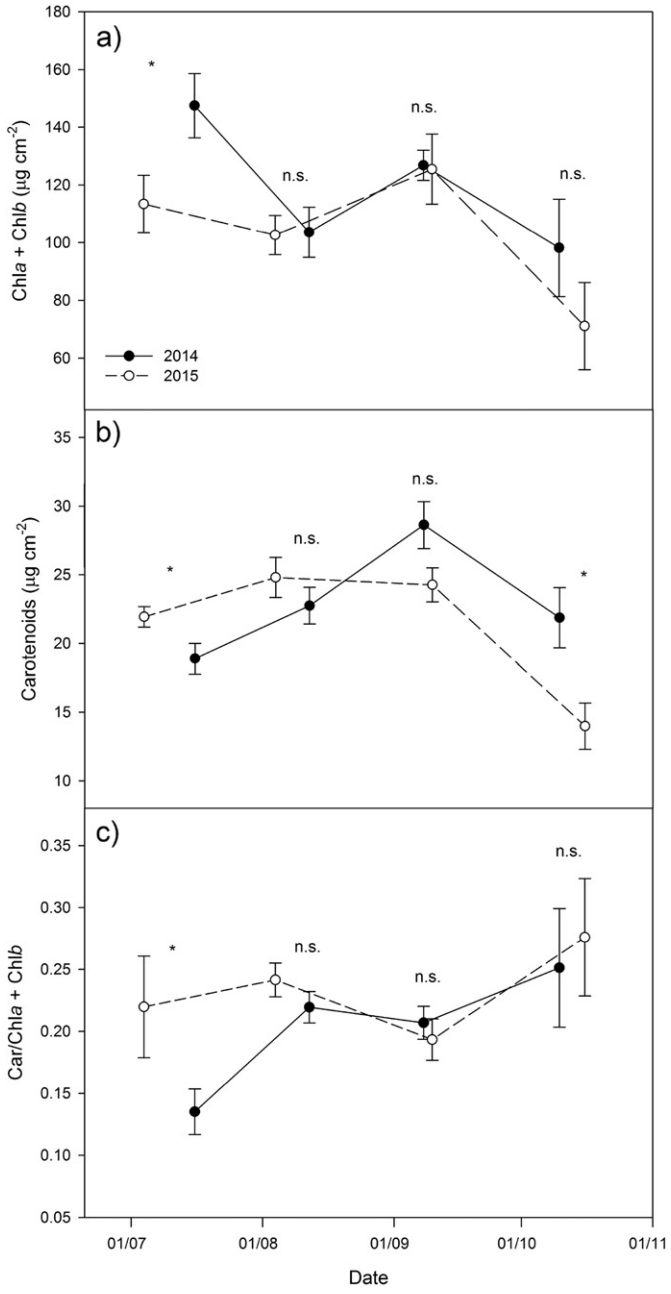


**Fig. 3.** Total chlorophyll (Chl *a* + Chl *b*; Chl tot) (a), carotenoids (Car) (b) and carotenoids to total chlorophyll (Car/Chl tot) ratio (c) in leaves of *Fagus sylvatica* L. collected at Collelongo beech forest during the growing season 2014 (black circles) and 2015 (white circles). Leaves were collected at the top of the canopy (26 m). Each value represents the mean of at least three measurements for branch of six labelled trees ($n = 12–18$) ± standard error. For each month, asterisks represent significantly different data (*t*-test, $P \leq 0.05$; n.s. = not significant, * ≤ 0.05).

leaf. In our study, *chlorophyll* indices were better related to N content, than to Chl tot, possibly because of different number of replicates and sampling procedures performed for Chl and N analyses.

*3.3.2. Fluorescence parameters*

The actual photon yield of PSII photochemistry in the light ($\Phi_{PSII}$) was significantly higher in July 2014 than July 2015, while during the other campaigns no significant differences were observed (Fig. 5a). The lower $\Phi_{PSII}$ in July 2015 was associated with a higher non-radiative energy dissipation (NRD) capacity, as shown by the non-photochemical quenching (NPQ) trend (Fig. 5b,c). Inter-annual and seasonal changes of $\Phi_{PSII}$ were reflected in changing photosynthetic electron transport rate (ETR) and NPQ (Fig. 5b,c). Particularly, ETR was higher and NPQ lower in July 2014 than July 2015. These results indicated that, during the relatively hot and dry July 2015, plants reduced the photosynthetic electron transport and increased the proportion of absorbed energy to be dissipated as heat in order to avoid photoinhibition and photodamage on PSII, as previously observed in populations of beech seedlings subjected to water deficit (Cocozza et al., 2016; Pšidová et al., 2015). In October, ETR decreased in both years due to the onset of senescence phase. However, in 2015 a more marked decrease of ETR and a higher NPQ were observed (Fig. 5b,c). We found significant correlations between ETR and all the *structural* and *chlorophyll* indices (Table 3). The best relationships were found for EVI 2, RDVI, DVI and MCARI 1 (Table 3), which are the same indices (*structural*) that better tracked NEE in 2014 (Table 2). This result could be partly explained by the fact that this relationship is mainly driven by the changes in canopy structure (LAI and canopy coverage) occurring during the final part of the vegetative period, when we recorded a rapid drop of both canopy (NEE) and leaf level (ETR) measurements. Accordingly, ETR determined by chlorophyll fluorescence showed a significant positive relationship with NEE ($R^2 = 0.79$; $P = 0.0006$).

*3.4. Carotenoid spectral indices as indicators of stress and senescence*

The PSRI index was first proposed by Merzlyak et al. (1999) as being sensitive to the senescence phase of plant development. In our study, monthly average PSRI increased progressively from July to October 2014 (Fig. 6a), in line with the ontogenetic stages of the canopy. On the contrary, PSRI values resulted almost stable from July to September 2015, while sharply increasing during October of the same year with the onset of the senescence phase (Fig. 6a). However, it is noteworthy that the PSRI values were significantly higher in 2015 than in 2014 reflecting the photosynthetic pigment composition (Figs. 3 and 4), as confirmed by the strong relationships between PSRI with Chl tot, Car/Chl tot and VAZ (Table 3 and Section 3.3). The lower net $CO_2$ uptake and ETR in October 2015 than October 2014 support the evidence of an anticipated senescence (Figs. 2 and 5), also suggested by the general lower content of carotenoids, the faster and more consistent reduction of the xanthophylls pool and higher PSRI values in this month (Figs. 3b, 4, 6). Moreover, if the senescence phase (October) is excluded, a significant relationship between PSRI and SWC can be observed (Fig. 6a, insert), suggesting that when the changes in pigment composition of the canopy is not dependent on the senescence, this VI is sensitive to variations of soil moisture. These results are in agreement with previous studies showing that PSRI is a valuable proxy in determining secondary effects of water stress (Struthers et al., 2013).

While on a diurnal time scale PRI responds to xanthophyll cycle variations (Wong and Gamon, 2015a, b), in our two years-study we focused on the seasonal time scale when PRI is mainly driven by pigment transformations associated with ontogeny and not by the xanthophyll cycle per se (Gitelson et al., 2017a).

The monthly averages of the PRI index showed a seasonal trend, with a decrease during the senescence phase in October of both years (Fig. 6b). Moreover, the PRI in 2014 resulted lower than 2015 in July ($P < 0.01$), September ($P < 0.0001$) and October ($P < 0.05$), while there was not significant difference in August (Fig. 6b). These results suggest that PRI is an indicator of seasonal changes in leaf pigment composition (mainly chlorophylls, carotenoids and anthocyanins), and hence of photosynthetic activity (Gitelson et al., 2017b), in line with the lower sink capacity of the forest in July and October 2015 compared to the same period in 2014 (Fig. 2). The PRI-Chl tot relationship was stronger than PRI-Car (Table 3), as previously observed for beech leaves (Gitelson et al., 2017a); anyway, the PRI correlation with the VAZ fraction of total carotenoids was high, confirming the link of this index to the size of the xanthophylls cycle pigment pool (Gamon et al., 1997; Gitelson et al., 2017a). The differences in fluorescence parameters and in Car/Chl tot ratio between July 2014 and July 2015 also reflected significant

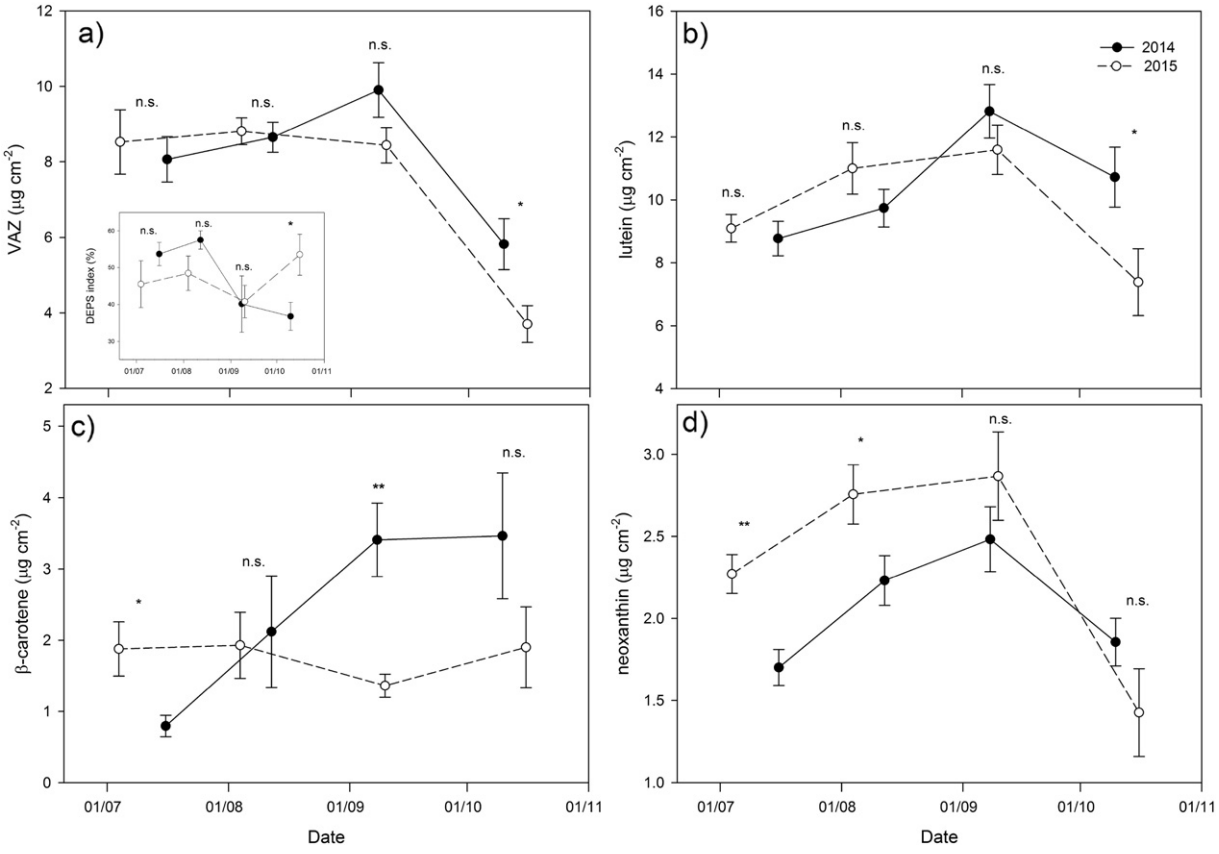


**Fig. 4.** Leaf contents of VAZ (Violaxanthin + Antheraxanthin + Zeaxanthin) pool (a), lutein (b), β-carotene (c) and neoxanthin (d) in the beech forest of Collelongo during the two growing seasons 2014 (black circles) and 2015 (white circles). Each value represents three measurements for branch of six labelled trees ($n = 12–18$) ± standard error. The insert shown in panel c represents the de-epoxidation index (DEPS, [(A/2) + Z]/(V + A + Z)). For each month, asterisks indicate significantly different data (*t*-test, $P \leq 0.05$); n.s. = not significant, * ≤ 0.05, ** ≤ 0.01.

variations in PRI values between the two growing seasons (compare Figs. 3, 5 and 6), indicating that this index is able to detect changes in leaf pigment composition and energy dissipation mechanism associated with dry and hot periods.

Merlier et al. (2015) and Hmimina et al. (2015) suggested that PRI variability can be distinguished into two components: a constitutive one linked to the canopy Chl content and pigment composition, and a physiological one linked to both pigment composition and soil moisture. In agreement with these studies, we reported significant relationships between PRI with both Chl and Car content throughout the season (Table 3) and between PRI and SWC when the senescence period was excluded by the analysis (Fig. 6b, insert). These data support the hypothesis that, when pigment composition is not affected by the senescence phase, the plant physiological status and the environmental factors (stress response to reduced SWC) become the main drivers of PRI variability (Inoue and Peñuelas, 2006; Merlier et al., 2015; Sarlikioti et al., 2010).

## 4. Conclusions

Our study focused on exploring the functionality of a Mediterranean-montane beech forest over two years with different stress conditions using various methods from canopy to leaf level. We investigated seasonal patterns of meteorological data, C fluxes, photosynthetic pigments and chlorophyll fluorescence, which consistently confirmed a hot and dry period in July 2015 and an earlier senescence in October 2015 compared to 2014. Our results led to the following conclusions.

- VIs related to structure (EVI 2, RDVI, DVI and MCARI 1) were found to better predict NEE changes for 2014, while those related to chlorophyll (SR red edge, CL red edge, MTCI and DR) provided better performances for 2015. This suggests that when forest sink capacity is not limited by environmental conditions, phenology (e.g. timing of foliage development and maturity) and structural parameters (e.g. development and layering of leaf area) are the main drivers of the C uptake capacity; conversely, when stress events occurr during the growing season, the shifting in pigment composition with the related effects on leaf physiology becomes one of the key factors of the ecophysiological forest dynamics. Thus, our study supports the use of red edge indices for estimation of plant stress physiology.
- Both *structural* and *chlorophyll* indices correlated with biochemical and physiological leaf-traits associated with the photosynthetic performance of top-canopy layer, such as ETR determined by fluorescence measurements, leaf Chl, carotenoid and N contents. However, the *chlorophyll* indices were more tightly connected to N, while the *structural* ones tracked the ETR seasonal trend mediated by the canopy structural changes occurring during the senescence period.
- Most of the *chlorophyll* indices investigated significantly correlated with Chls and carotenoids, but PSRI and PRI were the only spectral indices that correlated with both Chl tot, carotenoids and VAZ. These indices were good proxies of the variations in photosynthetic pigment composition related to changes in soil moisture (July–September) and senescence (October).

Overall, our study supports the hypothesis that a combination of different methodological approaches for the evaluation of plant functional and structural traits can provide detailed information on the main processes affecting forest C dynamics, also under stress conditions. This is of

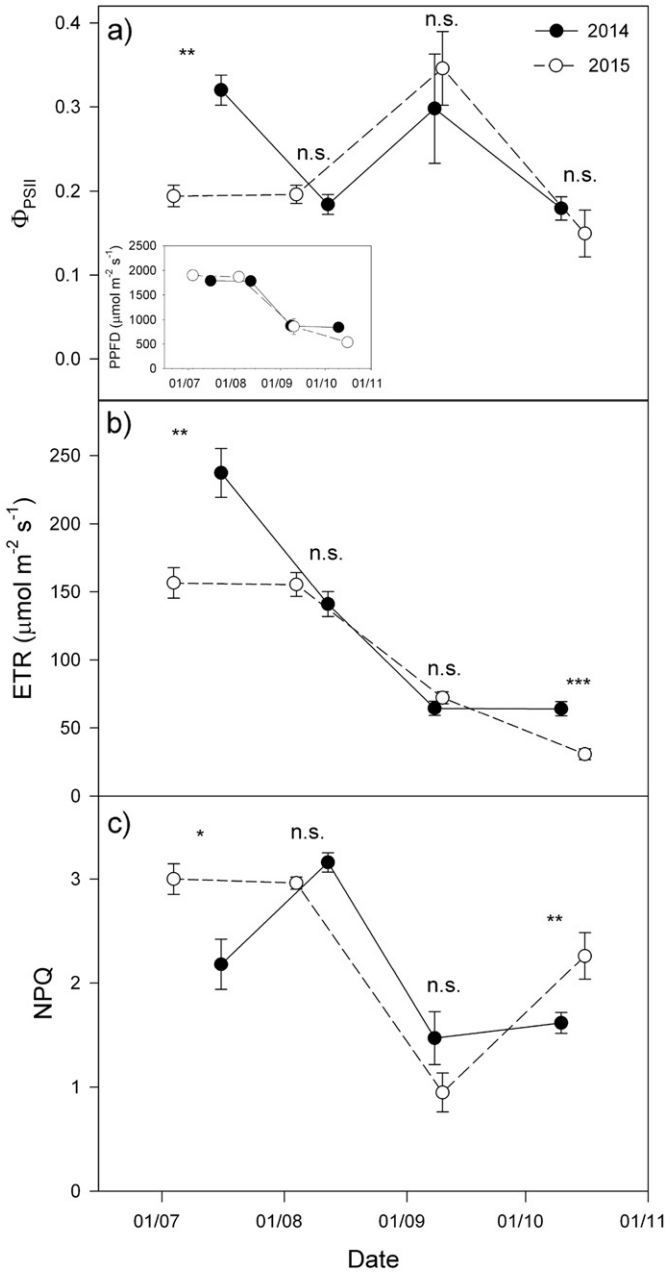


**Fig. 5.** The fluorescence-derived actual photochemical efficiency of PSII ($\Phi_{PSII}$) (a), electron transport rate (ETR) (b) and non-photochemical quenching (NPQ) (c) in leaves collected at Collelongo beech forest during the growing season 2014 (black circles) and 2015 (white circles). Each value represents the mean of at least 20 leaf fluorescence measuements ± standard error. The insert shown in panel a represents the average values of photosynthetic photon flux density (PPFD). For each month, asterisks indicate significantly different data (*t*-test, $P \le 0.05$); n.s. = not significant, * ≤ 0.05, ** ≤ 0.01, *** ≤ 0.001.

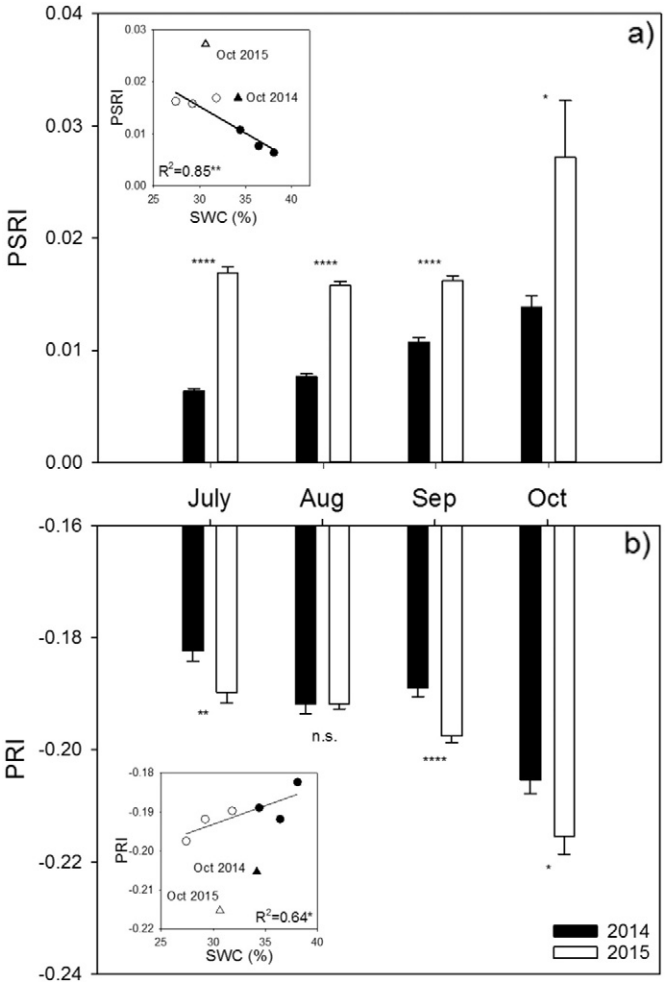


**Fig. 6.** Seasonal trend of PSRI (a) and PRI (b) for 2014 (black bars) and 2015 (white bars). Data shown are monthly averages ($n$ = 12–31) ± standard error. Asterisks indicate significantly different data (*t*-test, $P \le 0.05$); n.s. = not significant, * ≤ 0.05, ** ≤ 0.01, **** ≤ 0.0001. Inserts: correlations between PRSI (panel a) or PRI (panel b) and SWC (%). Black and white circles represent year 2014 and 2015, respectively. The coefficient of determination ($R^2$) refers to the period July–September. October values (out of relations) are presented as black and white triangles for 2014 and 2015, respectively.

considerable interest if, as expected, climate change will increase the frequency and intensity of heat and drought events, with potential strong implications on C sink capacity of forest ecosystems.

## Acknowledgments

This research was supported by the NextData MIUR-CNR project of interest, H2020 EcoPotential (grant agreement No. 641762), eLTER H2020 (GA n. 654359), MIUR-PRIN 2012 2012E3F3LK, PON I-AMICA (GA n. PONa3_00363) and PALMO projects. Collelongo-Selva Piana is a site of the Italian Long Term Ecological Research network (LTER Italy) and of the CONECOFOR and ICP-Forests forest monitoring programmes.

The authors thank Gregorio Sgrigna, Guglielmo Santi, Luca Tosi, Chris Mollica, Luca Leonardi, and Federico Leoni for field sampling support. We are thankful to Floriano Di Nardo for the help in the maintenance of eddy covariance tower and to Giovanni De Simoni and Floriano Di Nardo for mounting the radiometer on the flux tower. We also thank Del Nantt from Cropscan, Inc. for technical assistance on multispectral radiometer and Woody Clarke for english editing.

## Appendix A. Supplementary data

Supplementary data to this article can be found online at http://dx.doi.org/10.1016/j.scitotenv.2017.08.167.

## References

Aubinet, M., Grelle, A., Ibrom, A., Rannik, Ü., Moncrieff, J., Foken, T., Kowalski, A.S., Martin, P.H., Berbigier, P., Bernhofer, C., Clement, R., Elbers, J., Granier, A., Grünwald, T., Morgenstern, K., Pilegaard, K., Rebmann, C., Snijders, W., Valentini, R., Vesala, T., 1999. Estimates of the annual net carbon and water exchange of forests: the EUROFLUX methodology. Adv. Ecol. Res. 30:113–175. http://dx.doi.org/10.1016/S0065-2504(08)60018-5.

Baker, N.R., 2008. Chlorophyll fluorescence: a probe of photosynthesis in vivo. Annu. Rev. Plant Biol. 59:89–113. http://dx.doi.org/10.1146/annurev.arplant.59.032607.092759.

Balzarolo, M., Vescovo, L., Hammerle, A., Gianelle, D., Papale, D., Tomelleri, E., Wohlfahrt, G., 2015. On the relationship between ecosystem-scale hyperspectral reflectance

and $CO_2$ exchange in European mountain grasslands. Biogeosciences 12:3089–3108. http://dx.doi.org/10.5194/bg-12-3089-2015.
Bilger, W., Björkman, O., 1990. Role of the xanthophyll cycle in photoprotection elucidated by measurements of light-induced absorbance changes, fluorescence and photosynthesis in leaves of Hedera canariensis. Photosynth. Res. 25:173–185. http://dx.doi.org/10.1007/BF00033159.
Blackburn, G.A., 1998. Spectral indices for estimating photosynthethic pigment concentrations: a test using senescent tree leaves. Int. J. Remote Sens. 19:657–675. http://dx.doi.org/10.1080/014311698215919.
Carter, G.A., Miller, R.L., 1994. Early detection of plant stress by digital imaging within narrow stress-sensitive wavebands. Remote Sens. Biosph. Funct. 50, 295–301.
Castagna, A., Di Baccio, D., Tognetti, R., Ranieri, A., Sebastiani, L., 2013. Differential ozone sensitivity interferes with cadmium stress in poplar clones. Biol. Plant. 57:313–324. http://dx.doi.org/10.1007/s10535-012-0274-0.
Chatfield, C., 2016. The Analysis of Time Series: An Introduction. Sixth ed. CRC Press, Taylor and Francis Group, New York.
Clevers, J.G.P.W., Kooistra, L., 2012. Using hyperspectral remote sensing data for retrieving canopy chlorophyll and nitrogen content. IEEE J. Sel. Top. Appl. Earth Obs. Remote Sens. 5:574–583. http://dx.doi.org/10.1109/JSTARS.2011.2176468.
Cocozza, C., de Miguel, M., Pšidová, E., Ditmarová, L., Marino, S., Maiuro, L., Alvino, A., Czajkowski, T., Bolte, A., Tognetti, R., 2016. Variation in ecophysiological traits and drought tolerance of beech (*Fagus sylvatica* L.) seedlings from different populations. Front. Plant Sci. 7:886. http://dx.doi.org/10.3389/fpls.2016.00886.
Coops, N.C., Ferster, C.J., Waring, R.H., Nightingale, J., 2009. Comparison of three models for predicting gross primary production across and within forested ecoregions in the contiguous United States. Remote Sens. Environ. 113:680–690. http://dx.doi.org/10.1016/j.rse.2008.11.013.
Dall'Osto, L., Lico, C., Alric, J., Giuliano, G., Havaux, M., Bassi, R., 2006. Lutein is needed for efficient chlorophyll triplet quenching in the major LHCII antenna complex of higher plants and effective photoprotection in vivo under strong light. BMC Plant Biol. 6:32. http://dx.doi.org/10.1186/1471-2229-6-32.
Dani, K.G.S., Fineschi, S., Michelozzi, M., Loreto, F., 2016. Do cytokinins, volatile isoprenoids and carotenoids synergically delay leaf senescence? Plant Cell Environ. 39:1103–1111. http://dx.doi.org/10.1111/pce.12705.
Danielewska, A., Clarke, N., Olejnik, J., Hansen, K., de Vries, W., Lundin, L., Tuovinen, Juha-Pekka Fischer, R., Marek, U., Paoletti, E., 2013. A meta-database comparison from various European Research and Monitoring Networks dedicated to forest sites. iForest 6: 1–9. http://dx.doi.org/10.3832/ifor0751-006.
Dash, J., Curran, P.J., 2004. The MERIS terrestrial chlorophyll index. Int. J. Remote Sens. 25: 5403–5413. http://dx.doi.org/10.1080/0143116042000274015.
Datt, B., 1999. A new reflectance index for remote sensing of chlorophyll content in higher plants: tests using eucalyptus leaves. J. Plant Physiol. 154:30–36. http://dx.doi.org/10.1016/S0176-1617(99)80314-9.
Demmig-Adams, B., Adams, W.W., 2006. Photoprotection in an ecological context: the remarkable complexity of thermal energy dissipation. New Phytol. 172:11–21. http://dx.doi.org/10.1111/j.1469-8137.2006.01835.x.
Demming-Adams, B., Adams, W.W., 1996. The role of xanthophyll cycle carotenoids in the protection of photosynthesis. Trends Plant Sci. 1:21–26. http://dx.doi.org/10.1016/S1360-1385(96)80019-7.
Di Baccio, D., Castagna, A., Tognetti, R., Ranieri, A., Sebastiani, L., 2014. Early responses to cadmium of two poplar clones that differ in stress tolerance. J. Plant Physiol. 171: 1693–1705. http://dx.doi.org/10.1016/j.jplph.2014.08.007.
Dong, J., Xiao, X., Wagle, P., Zhang, G., Zhou, Y., Jin, C., Torn, M.S., Meyers, T.P., Suyker, A.E., Wang, J., Yan, H., Biradar, C., Moore, B., 2015. Comparison of four EVI-based models for estimating gross primary production of maize and soybean croplands and tallgrass prairie under severe drought. Remote Sens. Environ. 162:154–168. http://dx.doi.org/10.1016/j.rse.2015.02.022.
Gamon, J.A., 2015. Reviews and syntheses: optical sampling of the flux tower footprint. Biogeosciences 12:4509–4523. http://dx.doi.org/10.5194/bg-12-4509-2015.
Gamon, J.A., Peñuelas, J., Field, C.B., 1992. A narrow-waveband spectral index that tracks diurnal changes in photosynthetic efficiency. Remote Sens. Environ. 41:35–44. http://dx.doi.org/10.1016/0034-4257(92)90059-S.
Gamon, J.A., Field, C.B., Goulden, M.L., Griffin, K.L., Hartley, A.E., Joel, G., Peñuelas, J., Valentini, R., 1995. Relationships between NDVI, canopy structure, and photosynthesis in three Californian vegetation types. Ecol. Appl. 5:28–41. http://dx.doi.org/10.2307/1942049.
Gamon, A., Serrano, L., Surfus, S., 1997. The photochemical refectance index: an optical indicator of photosynthetic radiation use efficiency across species, functional types, and nutrient levels. Oecologia 112:492–501. http://dx.doi.org/10.1007/s004420050337.
Gamon, J.A., Coburn, C., Flanagan, L.B., Huemmrich, K.F., Kiddle, C., Sanchez-Azofeifa, G.A., Thayer, D.R., Vescovo, L., Gianelle, D., Sims, D.A., Rahman, A.F., Pastorello, G.Z., 2010. SpecNet revisited: bridging flux and remote sensing communities. Can. J. Remote. Sens. 36:S376–S390. http://dx.doi.org/10.5589/m10-067.
Garbulsky, M.F., Peñuelas, J., Gamon, J., Inoue, Y., Filella, I., 2011. The photochemical reflectance index (PRI) and the remote sensing of leaf, canopy and ecosystem radiation use efficiencies. A review and meta-analysis. Remote Sens. Environ. 115:281–297. http://dx.doi.org/10.1016/j.rse.2010.08.023.
Garbulsky, M.F., Peñuelas, J., Ogaya, R., Filella, I., 2013. Leaf and stand-level carbon uptake of a Mediterranean forest estimated using the satellite-derived reflectance indices EVI and PRI. Int. J. Remote Sens. 34:1282–1296. http://dx.doi.org/10.1080/01431161.2012.718457.
García-Plazaola, J., Matsubara, S., Osmond, C.B., 2007. The lutein epoxide cycle in higher plants: its relationships to other xanthophyll cycles and possible functions. Funct. Plant Biol. 34:759–773. http://dx.doi.org/10.1016/j.bbabio.2011.04.012.
Gitelson, A.A., 2003. Remote estimation of leaf area index and green leaf biomass in maize canopies. Geophys. Res. Lett. 30:4–7. http://dx.doi.org/10.1029/2002GL016450.
Gitelson, A.A., 2004. Wide Dynamic Range Vegetation Index for remote quantification of biophysical characteristics of vegetation. J. Plant Physiol. 161:165–173. http://dx.doi.org/10.1078/0176-1617-01176.
Gitelson, A., Merzlyak, M.N., 1994. Quantitative estimation of chlorophyll-a using reflectance spectra: experiments with autumn chestnut and maple leaves. J. Photochem. Photobiol. B Biol. 22:247–252. http://dx.doi.org/10.1016/1011-1344(93)06963-4.
Gitelson, A.A., Merzlyak, M.N., 1996. Signature analysis of leaf reflectance spectra: algorithm development for remote sensing of chlorophyll. J. Plant Physiol. http://dx.doi.org/10.1016/S0176-1617(96)80284-7.
Gitelson, A., Merzlyak, M.N., 1997. Remote estimation of chlorophyll content in higher plant leaves. Int. J. Remote Sens. 18:2691–2697. http://dx.doi.org/10.1080/014311697217558.
Gitelson, A.A., Kaufman, Y.J., Merzlyak, M.N., 1996. Use of a green channel in remote sensing of global vegetation from EOS-MODIS. Remote Sens. Environ. 58:289–298. http://dx.doi.org/10.1016/S0034-4257(96)00072-7.
Gitelson, A.A., Zur, Y., Chivkunova, O.B., Merzlyak, M.N., 2002. Assessing carotenoid content in plant leaves with reflectance spectroscopy. Photochem. Photobiol. 75: 272–281. http://dx.doi.org/10.1562/0031-8655(2002)0750272ACCIPL2.0.CO2.
Gitelson, A.A., Gritz, Y., Merzlyak, M.N., 2003. Relationships between leaf chlorophyll content and spectral reflectance and algorithms for non-destructive chlorophyll assessment in higher plant leaves. J. Plant Physiol. 160:271–282. http://dx.doi.org/10.1078/0176-1617-00887.
Gitelson, A.A., Viña, A., Ciganda, V., Rundquist, D.C., Arkebauer, T.J., 2005. Remote estimation of canopy chlorophyll content in crops. Geophys. Res. Lett. 32:1–4. http://dx.doi.org/10.1029/2005GL022688.
Gitelson, A.A., Gamon, J.A., Solovchenko, A., 2017a. Multiple drivers of seasonal change in PRI: implications for photosynthesis 1. Leaf level. Remote Sens. Environ. 191: 110–116. http://dx.doi.org/10.1016/j.rse.2016.12.014.
Gitelson, A.A., Gamon, J.A., Solovchenko, A., 2017b. Multiple drivers of seasonal change in PRI: implications for photosynthesis 2. Stand level. Remote Sens. Environ. 190: 198–206. http://dx.doi.org/10.1016/j.rse.2016.12.015.
Glenn, E.P., Huete, A.R., Nagler, P.L., Nelson, S.G., 2008. Relationship between remotely-sensed vegetation indices, canopy attributes and plant physiological processes: what vegetation indices can and cannot tell us about the landscape. Sensors 8: 2136–2160. http://dx.doi.org/10.3390/s8042136.
Gower, S.T., Kucharik, C.J., Norman, J.M., 1999. Direct and indirect estimation of leaf area index, fAPAR, and net primary production of terrestrial ecosystems. Remote Sens. Environ. 70:29–51. http://dx.doi.org/10.1016/S0034-4257(99)00056-5.
Guidolotti, G., Rey, A., D'Andrea, E., Matteucci, G., De Angelis, P., 2013. Effect of environmental variables and stand structure on ecosystem respiration components in a Mediterranean beech forest. Tree Physiol. 33:960–972. http://dx.doi.org/10.1093/treephys/tpt065.
Haboudane, D., Miller, J.R., Tremblay, N., Zarco-Tejada, P.J., Dextraze, L., 2002. Integrated narrow-band vegetation indices for prediction of crop chlorophyll content for application to precision agriculture. Remote Sens. Environ. 81:416–426. http://dx.doi.org/10.1016/S0034-4257(02)00018-4.
Haboudane, D., Miller, J.R., Pattey, E., Zarco-Tejada, P.J., Strachan, I.B., 2004. Hyperspectral vegetation indices and novel algorithms for predicting green LAI of crop canopies: modeling and validation in the context of precision agriculture. Remote Sens. Environ. 90:337–352. http://dx.doi.org/10.1016/j.rse.2003.12.013.
Hmimina, G., Dufrêne, E., Soudani, K., 2014. Relationship between photochemical reflectance index and leaf ecophysiological and biochemical parameters under two different water statuses: towards a rapid and efficient correction method using real-time measurements. Plant Cell Environ. 37:473–487. http://dx.doi.org/10.1111/pce.12171.
Hmimina, G., Merlier, E., Dufrêne, E., Soudani, K., 2015. Deconvolution of pigment and physiologically related photochemical reflectance index variability at the canopy scale over an entire growing season. Plant Cell Environ. 38:1578–1590. http://dx.doi.org/10.1111/pce.12509.
Horler, D.N.H., Dockray, M., Barber, J., Barringer, A.R., 1983. Red edge measurements for remotely sensing plant chlorophyll content. Adv. Space Res. 3:273–277. http://dx.doi.org/10.1016/0273-1177(83)90130-8.
Huemmrich, K.F., Gamon, J.A., Tweedie, C.E., Oberbauer, S.F., Kinoshita, G., Houston, S., Kuchy, A., Hollister, R.D., Kwon, H., Mano, M., Harazono, Y., Webber, P.J., Oechel, W.C., 2010. Remote sensing of tundra gross ecosystem productivity and light use efficiency under varying temperature and moisture conditions. Remote Sens. Environ. 114:481–489. http://dx.doi.org/10.1016/j.rse.2009.10.003.
Huete, A., Didan, K., Miura, T., Rodriguez, E.P., Gao, X., Ferreira, L.G., 2002. Overview of the radiometric and biophysical performance of the MODIS vegetation indices. Remote Sens. Environ. 83:195–213. http://dx.doi.org/10.1016/S0034-4257(02)00096-2.
Inoue, Y., Peñuelas, J., 2006. Relationship between light use efficiency and photochemical reflectance index in soybean leaves as affected by soil water content. Int. J. Remote Sens. 27:5109–5114. http://dx.doi.org/10.1080/01431160500373039.
Inoue, Y., Peñuelas, J., Miyata, A., Mano, M., 2008. Normalized difference spectral indices for estimating photosynthetic efficiency and capacity at a canopy scale derived from hyperspectral and $CO_2$ flux measurements in rice. Remote Sens. Environ. 112: 156–172. http://dx.doi.org/10.1016/j.rse.2007.04.011.
Jiang, Z., Huete, A., Didan, K., Miura, T., 2008. Development of a two-band enhanced vegetation index without a blue band. Remote Sens. Environ. 112:3833–3845. http://dx.doi.org/10.1016/j.rse.2008.06.006.
Jordan, C.F., 1969. Derivation of leaf-area index from quality of light on the forest floor. Ecology 50:663–666. http://dx.doi.org/10.2307/1936256.
Le Maire, G., Davi, H., Soudani, K., François, C., Le Dantec, V., Dufrêne, E., 2005. Modeling annual production and carbon fluxes of a large managed temperate forest using forest inventories, satellite data and field measurements. Tree Physiol. 25:859–872. http://dx.doi.org/10.1093/treephys/25.7.859.

Long, S.P., Bernacchi, C.J., 2003. Gas exchange measurements, what can they tell us about the underlying limitations to photosynthesis? Procedures and sources of error. J. Exp. Bot. 54:2393–2401. http://dx.doi.org/10.1093/jxb/erg262.

Main, R., Azong, M., Mathieu, R., Kennedy, M.M.O., Ramoelo, A., Koch, S., 2011. An investigation into robust spectral indices for leaf chlorophyll estimation. ISPRS J. Photogramm. Remote Sens. 66:751–761. http://dx.doi.org/10.1016/j.isprsjprs.2011.08.001.

Matteucci, G., Masci, A., Valentini, R., Scarascia, G., 2007. The Response of Forests to Global Change: Measurements and Modelling Simulations in a Mountain Forest of the Mediterranean Region. In: Palahi, M., Byrot, Y., Rois, M. (Eds.), Scientific Tools and Research Needs for Multifunctional Mediterranean Forest Ecosystem Management. EFI Proceedings, Joensuu, Finland, pp. 11–23.

Maxwell, K., Johnson, G.N., 2000. Chlorophyll fluorescence-a practical guide. J. Exp. Bot. 51:659–668. http://dx.doi.org/10.1093/jexbot/51.345.659.

Mazzenga, F., 2017. Analisi di lungo termine sui fattori di controllo dello scambio di carbonio in una faggeta dell' Italia centromeridionale. (PhD Thesis). Department for Innovation in Biological, Agro-food and Forest systems. University of Tuscia, Viterbo, Italy.

Merlier, E., Hmimina, G., Dufrêne, E., Soudani, K., 2015. Explaining the variability of the photochemical reflectance index (PRI) at the canopy-scale: disentangling the effects of phenological and physiological changes. J. Photochem. Photobiol. B Biol. 151: 161–171. http://dx.doi.org/10.1016/j.jphotobiol.2015.08.006.

Meroni, M., Panigada, C., Rossini, M., Picchi, V., Cogliati, S., Colombo, R., 2009. Using optical remote sensing techniques to track the development of ozone-induced stress. Environ. Pollut. 157:1413–1420. http://dx.doi.org/10.1016/j.envpol.2008.09.018.

Merzlyak, M.N., Gitelson, A.A., Chivkunova, O.B., Rakitin, V.Y.U., 1999. Non-destructive optical detection of pigment changes during leaf senescence and fruit ripening. Physiol. Plant. 106:135–141. http://dx.doi.org/10.1034/j.1399-3054.1999.106119.x.

Merzlyak, M.N., Solovchenko, A.E., Gitelson, A.A., 2003. Reflectance spectral features and non-destructive estimation of chlorophyll, carotenoid and anthocyanin content in apple fruit. Postharvest Biol. Technol. 27:197–211. http://dx.doi.org/10.1016/S0925-5214(02)00066-2.

Murchie, E.H., Lawson, T., 2013. Chlorophyll fluorescence analysis: a guide to good practice and understanding some new applications. J. Exp. Bot. http://dx.doi.org/10.1093/jxb/ert208.

Nakaji, T., Ide, R., Oguma, H., Saigusa, N., Fujinuma, Y., 2007. Utility of spectral vegetation index for estimation of gross $CO_2$ flux under varied sky conditions. Remote Sens. Environ. 109:274–284. http://dx.doi.org/10.1016/j.rse.2007.01.006.

Nestola, E., Calfapietra, C., Emmerton, C., Wong, C., Thayer, D., Gamon, J., 2016. Monitoring grassland seasonal carbon dynamics, by integrating MODIS NDVI, proximal optical sampling, and Eddy covariance measurements. Remote Sens. 8:260. http://dx.doi.org/10.3390/rs8030260.

Nestola, E., Sánchez-Zapero, J., Latorre, C., Mazzenga, F., Matteucci, G., Calfapietra, C., Camacho, F., 2017. Validation of PROBA-V GEOV1 and MODIS C5 & C6 fAPAR products in a deciduous beech Forest site in Italy. Remote Sens. 9:126. http://dx.doi.org/10.3390/rs9020126.

Ollinger, S.V., 2011. Sources of variability in canopy reflectance and the convergent properties of plants. New Phytol. 189:375–394. http://dx.doi.org/10.1111/j.1469-8137.2010.03536.x.

Papale, D., Reichstein, M., Aubinet, M., Canfora, E., Bernhofer, C., Kutsch, W., Longdoz, B., Rambal, S., Valentini, R., Vesala, T., Yakir, D., 2006. Towards a standardized processing of net ecosystem exchange measured with eddy covariance technique: algorithms and uncertainty estimation. Biogeosciences 3:571–583. http://dx.doi.org/10.5194/bg-3-571-2006.

Peng, Y., Gitelson, A.A., Keydan, G., Rundquist, D.C., Moses, W., 2011. Remote estimation of gross primary production in maize and support for a new paradigm based on total crop chlorophyll content. Remote Sens. Environ. 115:978–989. http://dx.doi.org/10.1016/j.rse.2010.12.001.

Pettorelli, N., Vik, J.O., Mysterud, A., Gaillard, J.M., Tucker, C.J., Stenseth, N.C., 2005. Using the satellite-derived NDVI to assess ecological responses to environmental change. Trends Ecol. Evol. 20:503–510. http://dx.doi.org/10.1016/j.tree.2005.05.011.

Pötzelsberger, E., Wolfslehner, B., Hasenauer, H., 2015. Climate change impacts on key forest functions of the Vienna Woods. Eur. J. For. Res. 481–496. http://dx.doi.org/10.1007/s10342-015-0866-2.

Procházková, D., Haisel, D., Wilhelmová, N., 2009. Content of carotenoids during ageing and senescence of tobacco leaves with genetically modulated life-span. Photosynthetica 47:409–414. http://dx.doi.org/10.1007/s11099-009-0062-z.

Pšidová, E., Ditmarová, Jamnická, G., Kurjak, D., Majerová, J., Czajkowski, T., Bolte, A., 2015. Photosynthetic response of beech seedlings of different origin to water deficit. Photosynthetica 53:187–194. http://dx.doi.org/10.1007/s11099-015-0101-x.

Ramoelo, A., Skidmore, A.K., Schlerf, M., Heitkönig, I.M.A., Mathieu, R., Cho, M.A., 2013. Savanna grass nitrogen to phosphorous ratio estimation using field spectroscopy and the potential for estimation with imaging spectroscopy. Int. J. Appl. Earth Obs. Geoinf. 23:334–343. http://dx.doi.org/10.1016/j.jag.2012.10.008.

Reichstein, M., Papale, D., Valentini, R., Aubinet, M., Bernhofer, C., Knohl, A., Laurila, T., Lindroth, A., Moors, E., Pilegaard, K., Seufert, G., 2007. Determinants of terrestrial ecosystem carbon balance inferred from European eddy covariance flux sites. Geophys. Res. Lett. 34:1–5. http://dx.doi.org/10.1029/2006GL027880.

Rock, B.N., Hoshizaki, T., Miller, J.R., 1988. Comparison of in situ and airborne spectral measurements of the blue shift associated with forest decline. Remote Sens. Environ. 24:109–127. http://dx.doi.org/10.1016/0034-4257(88)90008-9.

Rondeaux, G., Steven, M., Baret, F., 1996. Optimization of soil-adjusted vegetation indices. Remote Sens. Environ. 55:95–107. http://dx.doi.org/10.1016/0034-4257(95)00186-7.

Rossini, M., Cogliati, S., Meroni, M., Migliavacca, M., Galvagno, M., Busetto, L., Cremonese, E., Julitta, T., Siniscalco, C., Morra Di Cella, U., Colombo, R., 2012. Remote sensing-based estimation of gross primary production in a subalpine grassland. Biogeosciences 9:2565–2584. http://dx.doi.org/10.5194/bg-9-2565-2012.

Rouse, J.W., Haas, R.H., Schell, J.A., Deering, D.W., 1974. Monitoring vegetation systems in the Great Plains with ERTS. Third Earth Resources Technology Satellite-1 Symposium. NASA, Washington, DC, USA, pp. 309–317.

Sakowska, K., Vescovo, L., Marcolla, B., Juszczak, R., Olejnik, J., Gianelle, D., 2014. Monitoring of carbon dioxide fluxes in a subalpine grassland ecosystem of the Italian Alps using a multispectral sensor. Biogeosciences 11:4695–4712. http://dx.doi.org/10.5194/bg-11-4695-2014.

Sarlikioti, V., Driever, S.M., Marcelis, L.F.M., 2010. Photochemical reflectance index as a mean of monitoring early water stress. Ann. Appl. Biol. 157:81–89. http://dx.doi.org/10.1111/j.1744-7348.2010.00411.x.

Scartazza, A., Mata, C., Matteucci, G., Yakir, D., Moscatello, S., Brugnoli, E., 2004. Comparisons of $\delta^{13}C$ of photosynthetic products and ecosystem respiratory $CO_2$ and their responses to seasonal climate variability. Oecologia 140:340–351. http://dx.doi.org/10.1007/s00442-004-1588-1.

Scartazza, A., Moscatello, S., Matteucci, G., Battistelli, A., Brugnoli, E., 2013. Seasonal and inter-annual dynamics of growth, non-structural carbohydrates and C stable isotopes in a Mediterranean beech forest. Tree Physiol. 33:730–742. http://dx.doi.org/10.1093/treephys/tpt045.

Scartazza, A., Di Baccio, D., Bertolotto, P., Gavrichkova, O., Matteucci, G., 2016. Investigating the European beech (*Fagus sylvatica* L.) leaf characteristics along the vertical canopy profile: leaf structure, photosynthetic capacity, light energy dissipation and photoprotection mechanisms. Tree Physiol. 36:1060–1076. http://dx.doi.org/10.1093/treephys/tpw038.

Schlemmer, M., Gitelson, A., Schepers, J., Ferguson, R., Peng, Y., Shanahan, J., Rundquist, D., 2013. Remote estimation of nitrogen and chlorophyll contents in maize at leaf and canopy levels. Int. J. Appl. Earth Obs. Geoinf. 25:47–54. http://dx.doi.org/10.1016/j.jag.2013.04.003.

Scott, R.L., Huxman, T.E., Cable, W.L., Emmerich, W.E., 2006. Partitioning of evapotranspiration and its relation to carbon dioxide exchange in a Chihuahuan Desert shrubland. Hydrol. Process. 20:3227–3243. http://dx.doi.org/10.1002/hyp.6329.

Sims, D.A., Gamon, J.A., 2002. Relationships between leaf pigment content and spectral reflectance across a wide range of species,leaf structures and developmental stages. Remote Sens. Environ. 81:337–354. http://dx.doi.org/10.1016/S0034-4257(02)00010-X.

Struthers, R., Farifteh, J., Swennen, R., Coppin, P., 2013. Physiological and spectral response to water stress induced by regulated deficit irrigation on pear trees. Appl. Remote Sens. J. 3, 9–17.

Stylinski, C.D., Gamon, J.A., Oechel, W.C., 2002. Seasonal patterns of reflectance indices, carotenoid pigments and photosynthesis of evergreen chaparral species. Oecologia 131: 366–374. http://dx.doi.org/10.1007/s00442-002-0905-9.

Tucker, C.J., 1979. Red and photographic infrared linear combinations for monitoring vegetation. Remote Sens. Environ. 8:127–150. http://dx.doi.org/10.1016/0034-4257(79)90013-0.

Valentini, R., De Angelis, P., Matteuci, G., Monaco, R., Dore, S., Scarascia Mugnozza, G.E., 1996. Seasonal net carbon dioxide exchange of a beech forest with the atmosphere. Glob. Chang. Biol. 2:199–207. http://dx.doi.org/10.1111/j.1365-2486.1996.tb00072.x.

Vescovo, L., Wohlfahrt, G., Balzarolo, M., Pilloni, S., Sottocornola, M., Rodeghiero, M., Gianelle, D., 2012. New spectral vegetation indices based on the near-infrared shoulder wavelengths for remote detection of grassland phytomass. Int. J. Remote Sens. 33: 37–41. http://dx.doi.org/10.1080/01431161.2011.607195.

Wellburn, A., 1994. The spectral determination of chlorophyll a and chlorophyll b, as well as total carotenoids, using various solvents with spectrophotometers of different resolution. J. Plant Physiol. 144:307–313. http://dx.doi.org/10.1016/S0176-1617(11)81192-2.

Wong, C.Y.S., Gamon, J.A., 2015a. The photochemical reflectance index provides an optical indicator of spring photosynthetic activation in evergreen conifers. New Phytol. 206: 196–208. http://dx.doi.org/10.1111/nph.13251.

Wong, C.Y.S., Gamon, J.A., 2015b. Three causes of variation in the photochemical reflectance index (PRI) in evergreen conifers. New Phytol. 206:187–195. http://dx.doi.org/10.1111/nph.13159.

Wu, C., Niu, Z., Tang, Q., Huang, W., Rivard, B., Feng, J., 2009. Remote estimation of gross primary production in wheat using chlorophyll-related vegetation indices. Agric. For. Meteorol. 149:1015–1021. http://dx.doi.org/10.1016/j.agrformet.2008.12.007.

Wu, C., Han, X., Ni, J., Niu, Z., Huang, W., 2010a. Estimation of gross primary production in wheat from in situ measurements. Int. J. Appl. Earth Obs. Geoinf. 12:183–189. http://dx.doi.org/10.1016/j.jag.2010.02.006.

Wu, C., Munger, J.W., Niu, Z., Kuang, D., 2010b. Comparison of multiple models for estimating gross primary production using MODIS and eddy covariance data in Harvard Forest. Remote Sens. Environ. 114:2925–2939. http://dx.doi.org/10.1016/j.rse.2010.07.012.

Xiao, X., Zhang, Q., Braswell, B., Urbanski, S., Boles, S., Wofsy, S., Moore, B., Ojima, D., 2004. Modeling gross primary production of temperate deciduous broadleaf forest using satellite images and climate data. Remote Sens. Environ. 91:256–270. http://dx.doi.org/10.1016/j.rse.2004.03.010.

Zarco-Tejada, P.J., Miller, J.R., Noland, T.L., Mohammed, G.H., Sampson, P.H., 2001. Scaling-up and model inversion methods with narrowband optical indices for chlorophyll content estimation in closed forest canopies with hyperspectral data. IEEE Trans. Geosci. Remote Sens. 39:1491–1507. http://dx.doi.org/10.1109/36.934080.

Zarco-Tejada, P.J., Pushnik, J.C., Dobrowski, S., Ustin, S.L., 2003. Steady-state chlorophyll a fluorescence detection from canopy derivative reflectance and double-peak red-edge effects. Remote Sens. Environ. 84:283–294. http://dx.doi.org/10.1016/S0034-4257(02)00113-X.

Zarco-Tejada, P.J., Miller, J.R., Morales, A., Berjón, A., Agüera, J., 2004. Hyperspectral indices and model simulation for chlorophyll estimation in open-canopy tree crops. Remote Sens. Environ. 90:463–476. http://dx.doi.org/10.1016/j.rse.2004.01.017.